Master's thesis

NTNU
Norwegian University of Science and Technology
Faculty of Natural Sciences
Department of Biology

Pernille Sofie Moe

Investigating the effects of osmotic stress and cellulose biosynthesis inhibition on cell morphology and plasma membrane tension in *Arabidopsis thaliana* using confocal microscopy and the mechanosensitive Flipper-TR

Master's thesis in Biology
Supervisor: Thorsten Hamann
Co-supervisor: Luis Alonso Baez
May 2022

NTNU
Kunnskap for en bedre verden

Pernille Sofie Moe

Investigating the effects of osmotic stress and cellulose biosynthesis inhibition on cell morphology and plasma membrane tension in *Arabidopsis thaliana* using confocal microscopy and the mechanosensitive Flipper-TR

Master's thesis in Biology
Supervisor: Thorsten Hamann
Co-supervisor: Luis Alonso Baez
May 2022

Norwegian University of Science and Technology
Faculty of Natural Sciences
Department of Biology

NTNU
Norwegian University of
Science and Technology

Abstract

Plants, unable to flee from stress or danger due to their immobile existence, need a system to perceive and adapt to the environment. A cell wall surrounds the plant cell, giving structural and mechanical support to the plant. The cell wall integrity maintenance mechanism is enabling the plant cell to monitor the state of the cell wall during growth or environmental stress. Stress perception is therefore a prerequisite of cell adaption. The working hypothesis to be investigated here is that the plasma membrane, or components anchored to the plasma membrane are involved in stress perception, involving plasma membrane – cell wall continuum disruption.

To study visible effects of Isoxaben (ISX) and hyper-osmotic stress on *Arabidopsis thaliana* roots, seedlings expressing SYP121-YFP, which labels plasma membranes, were mock-, sorbitol-, ISX-, or ISX + sorbitol-treated. In addition, they were stained with propidium iodide to label cell walls and detect cell death. In accordance with other studies, sorbitol seems to hinder some of the effect ISX has on the cells, though there seems to be more cell death in ISX + Sorbitol-treated seedlings than in those treated only with ISX. To investigate what happens to plasma membrane tension in response to stress, fluorescence lifetime imaging microscopy was used to measure the lifetime of Flipper-TR in the epidermal plasma membrane of *Arabidopsis* seedlings. Flipper-TR has previously been used in mammalian cells and yeast cells but not in plants. Therefore, experimental conditions were first established before the effects of the same treatments as before were determined. ISX-treatments shorten the fluorescent lifetime compared to mock controls after around 4 hours. In contrast sorbitol-treatments increase the lifetime, also when combined with ISX, again implying sorbitol suppress the ISX effects on the seedling. Interestingly, the effect of hyper- and hypo-osmotic stress were found to have the opposite effect on the lifetime than what has been described previously in mammalian and yeast cells.

Sammendrag

Planter trenger et system for å oppfatte og tilpasse seg miljøet rundt, ettersom de ikke kan forflytte seg. Plantecellen er omgitt av en cellevegg som støtter opp planten strukturelt og mekanisk. Mekanismene for celleveggintegritetsvedlikehold gjør det mulig for plantecellen å overvåke celleveggens tilstand under vekst eller stress fra omgivelsene. Stresspersepsjon er derfor en viktig forutsetning for celletilpasning.

Hypotesen som undersøkes i denne oppgaven er at plasmamembranen, eller komponenter forankret i plasmamembranen, er involvert i stresspersepsjon, som involverer forstyrrelser i det fysiske forholdet mellom plasmamembran og celleveggen.

For å studere den synlige effekten av Isoxaben (ISX) og hyperosmotisk stress på *Arabidopsis thaliana* røtter, spirer som uttrykker SYP121-YFP, som merker plasmamembranen, ble kontroll-, sorbitol-, ISX- eller ISX + sorbitolbehandlet. Spirene var også farget med propidiumjodid for å farge celleveggen og observere celledød.

I overensstemmelse med tidligere studier virker det som om sorbitol demper noe av effekten ISX har på cellene, selv om det ser ut til å være mer celledød hos spirer behandlet med ISX + sorbitol enn spirene som kun er behandlet med ISX.

For å undersøke hva som skjer med plasmamembranspenningen i møte med stress ble fluorescens levetid mikroskopi (fluorescence lifetime imaging microscopy – FLIM) brukt til finne levetiden til Flipper-TR i *Arabidopsis* spirerenes plasmamembranen i epidermisceller. Flipper-TR har tidligere blitt brukt i dyreceller og gjærceller, men ikke i undersøkelser av planter. Forsøksbetingelser ble derfor først etablert før effekten av de tidligere nevnte behandlingene ble undersøkt. Resultatene av undersøkelsene viste at fire timer ISX-behandling gir en kortere fluorescens levetid sammenlignet med spirene som ble kontrollbehandlet. Til forskjell ga sorbitolbehandling en økning i levetid, også når det var i kombinasjon med ISX, som igjen antyder at sorbitol undertrykker effektene av ISX på spirene. Effekten av hyper-og hypo-osmotisk stress viste seg å ha motsatt effekt på fluorescens levetiden enn hva som tidligere har blitt observert i dyre- og gjærceller.

Acknowledgement

First, I would like to thank my supervisor Thorsten Hamann for the opportunity to be part of his research/lab group, for guidance, helpful insight, optimism and encouragement. A big thanks to my co-supervisor Luis Alonso Baez, for helping me in the search for the best experimental conditions, for being positive and always finding time to help me.
I would also express my gratitude to the rest of the lab, especially to Julia Schulz for helping me get started with this project. And many thanks to the other MSc students, Eline and Ruben, for the support, the help and for making this experience so much more entertaining.

Big thanks to Felicity Ashcroft for supplying me with HaCat cells, to Bjørnar Sporsheim at CMIC for helping me with the spectra, and to Astrid Bjørkøy for the training and continued help with the microscope every time there was a problem. Also, thanks Trude Johansen for help combating some experimental troubles.

Thanks to my fellow master students for the much-needed social lunch break and for establishing cake Friday so every week ended on a good note. Thank you Andreas, for being so encouraging and supporting through this time and for always making dinner when I got home late from an experiment. Lastly, I would like to thank friends and family for all their support and willingness to listen me talk about my thesis.

Table of Contents

List of figures

Appendix

Figure A.1: Line chart of mean lifetime and standard deviation for each treatment and timepoint

List of tables

Appendix

List of abbreviations

ABA	Abscisic acid
CESA	Cellulose synthase
CLSM	Confocal laser scanning microscopy
CrRLK1L	*Catharanthus roseus* RECEPTOR-LIKE KINASE1-LIKE
CSC	Cellulose synthase protein complexes
CWD	Cell wall damage
CWI	Cell wall integrity
DAMPs	Damage-Associated Molecular Patterns
DMEM	Dulbecco's modified Eagle Medium
DMSO	Dimethyl sulfoxid
DTT	Dithienothiophene
FBS	Fetal bovine serum
FCS	Fluorescence correlation spectroscopy
FER	FERONIA
FLIM	Fluorescence lifetime imaging microscopy
FRAP	Fluorescence recovery after photobleaching
FRET	Fluorescence resonance energy
GFP	Green fluorescent protein
GUVs	Giant unilamellar vesicles
HSD	Honestly Significant Difference
ISX	Isoxaben
JA	Jasmonic acid
Ld	Liquid disordered
Lo	Liquid ordered
MCA1	MID1 COMPLEMENTING ACTIVITY 1
MS	Murashige and Skoog
MSL10	MscS-like 10
OSCA1	REDUCED HYPEROSMOLALITY INDUCED CA2+ INCREASE 1
PAMPs	Pathogen-Associated Molecular Patterns
PBS	Phosphate buffered saline
PI	Propidium iodide

PM	Plasma membrane
PRRs	Pattern recognition receptors
RALFs	Rapid alkalinization factors
ROI	Region of interest
ROS	Reactive oxygen species
SA	Salicylic acid
SIM	Structured illumination microscopy
SPAD	Single photon avalanche diode
STED	Stimulated emission depletion
STORM	Stochastic optical reconstruction microscopy
TCSPC	Time-correlated single photon counting
THE1	THESEUS 1
TORC2	Target of rapamycin complex 2
WLL	White light laser
YFP	Yellow fluorescent protein

1. Introduction

With climate change giving rise to more extreme weather and less arable land, and the world population continuing to grow it is important to improve crop plants enabling them to withstand stress and continue growth despite unfavourable and challenging conditions (Aydinalp & Cresser, 2008; Gerland et al., 2014; Lesk et al., 2016). Flooding, drought, and salinization of soils are examples of the stresses plants face in the future (Aydinalp & Cresser, 2008; Lesk et al., 2016). Other unpredictable factors, such as war for instance, can also make food crops scarce in the countries affected as well as in their commercial partners / other countries, as recent time has shown.

One way of securing more food in the future is to make plants more resistant to different types of stress. To achieve this, it is important to know how plants normally respond to different environmental stress factors, and how the plasticity of the plants is regulated so that they can thrive in their place of growth. Then we can determine what is the best strategy to help plants to successfully adapt for the future.

1.1 The plant cell

The plant cell differs from an animal cell in various ways. One obvious difference is the cell wall that surrounds all plant cells and has very different mechanical characteristics compared to the extra-cellular matrices surrounding animal cells. Plant cells generate hydrostatic pressure by osmosis, called turgor pressure. The cell wall enables plants to generate this force, and turgor pressure is important for plant growth, development and response to stress (Pritchard, 2007). Animal cells do not have turgor pressure and their extracellular matrices cannot withstand high hydrostatic pressure therefore the cells are lysing when experiencing extreme hydrostatic pressures.

1.1.1 The cell wall

The plant cell wall has proven to be very important for people for thousands of years, as sources of e.g., food, textile and shelter, and will continue to be so in the future, as, for instance,

renewable materials and bioenergy will be more important moving forward (Anderson & Kieber, 2020).

The cell wall is surrounding the plasma membrane. The wall provides the plant with structural support to hold its own weight, to withstand (harsh) weather, and acts as first line of defense against biological interference. At the same time, it is important that the cell wall is able to change and be flexible during growth and in response to the environment (Anderson & Kieber, 2020). The plant cell wall is responsible for the shape of the cells, withstanding the turgor pressure, required for cell-cell adhesion and is therefore structurally and mechanistically important for the plant (Lee et al., 2011). Plasticity, the ability to change structure and composition in response to internal or external cues, is an important ability of the cell wall, as the cells change their form during development and when they have to adapt to biotic and abiotic stressors plants encounter during their life (Lampugnani et al., 2018).

Primary cell walls, which begin forming during cell division, consist of a network of polysaccharides such as cellulose, hemicellulose, pectin, and cell wall proteins (Sánchez-Rodríguez et al., 2010). Cellulose microfibrils are made up of β-1,4-linked glucan and are synthesized by cellulose synthase (CESA) protein complexes (CSC) (Persson et al., 2007). *Arabidopsis thaliana (*hereafter *Arabidopsis)* has 10 CESA isoforms, with 3 of them being responsible for primary cell wall cellulose synthesis, CESA1, CESA3 and CESA6 (Desprez et al., 2007). While CESA4, CESA7 and CESA8 synthesize cellulose for the secondary cell wall (Anderson & Kieber, 2020). The loadbearing cellulose microfibrils are cross-linked with hemicellulose and pectin (T. Wang et al., 2012). Common hemicelluloses in *Arabidopsis* are xyloglucans and xylans, with xyloglucans being more prominent in the primary cell wall and xylans being more prominent in secondary cell walls (Lampugnani et al., 2018). Pectins are polysaccharides containing galacturonic acid, with homogalacturonan being the most abundant, accounting for about 65% of pectin (Mohnen, 2008). Pectin functions include cell-cell adhesion, cell separation and signaling (Daher & Braybrook, 2015; Shin et al., 2021). Hemicellulose and pectins are (referred to as) matrix polysaccharides (Anderson & Kieber, 2020).

Many cells, influenced by their biological functions, develop a secondary cell wall after cell expansion stops and differentiation starts, e.g. xylem (Anderson & Kieber, 2020). The secondary cell wall contains different xylans, cellulose (synthesized by other CESAs involved

in the primary cell wall), and lignin (which is a waterproofing and strengthening organic polymer) (Somssich et al., 2016). Secondary cell walls are often thicker than primary cell walls and provide mechanical support to tissues and organs (Lee et al., 2011).

1.1.2 The plasma membrane

The plant plasma membrane (PM) consists mostly of lipids from three main classes; glycerolipids (mainly phospholipids), sterols, and sphingolipids, as well as proteins and carbohydrate groups attached to some of the proteins and lipids (Ackermann & Stanislas, 2020; Furt et al., 2011). The lipid-to-protein ratio is about 1, with lipid-to-protein molar ratio ranging from 50:1 to 100:1. A single cell can have over 1000 different lipid species (Furt et al., 2011). While the PM forms a selective barrier between the extracellular and intracellular, it is now viewed also as a dynamic signaling compartment and something that can help sense the mechanical state of the cells, with some cell wall sensors located at the PM, and possibly there are lipids that are direct sensors of the cell wall (Ackermann & Stanislas, 2020). An example of PM plasticity is the influence of heat stress. Plants can change membrane lipid metabolism under heat stress, and structural changes leading to membrane fluidity in the plasma membrane is one of the ways the plants can sense heat stress. It has been shown that it can lead to a decrease in phosphatidylethanolamine (a phospholipid), an increase in phosphatidylserine, phosphatidylinositol species and oxidized phospholipids (Higashi & Saito, 2019).

Experimentation, mostly in animal cells, has found that the PM is not homogenous, but rather that the membrane is compartmentalized and has so called microdomains. The microdomains differ in lipid and protein components compared to rest of the membrane, they are enriched in sterols and sphingolipids and specific proteins (Yu et al., 2020). Historically the difference in membrane composition laterally within the PM was supported by isolation of detergent-soluble and detergent-resistant membrane fractions (Furt et al., 2011; Yu et al., 2020). Several different fluorophores have been used to visualize and monitor microdomains in animal cells, but it has been a bit more difficult for plant cells because of the cell wall. More recently developments in microscopy technology, such as stimulated emission depletion (STED), structured illumination microscopy (SIM) and stochastic optical reconstruction microscopy (STORM), have made study of microdomains in plants easier. This can be coupled with fluorescent

reporter proteins fused to microdomains marker proteins, so dynamics and distributions of microdomains can be monitored (Yu et al., 2020).

The membrane can also be divided into two phases, a liquid ordered phase (L_o) with saturated lipid species and cholesterol that is packed, and a liquid disordered phase (L_d) with mainly unsaturated lipids (Gronnier et al., 2018), se figure 1.1.

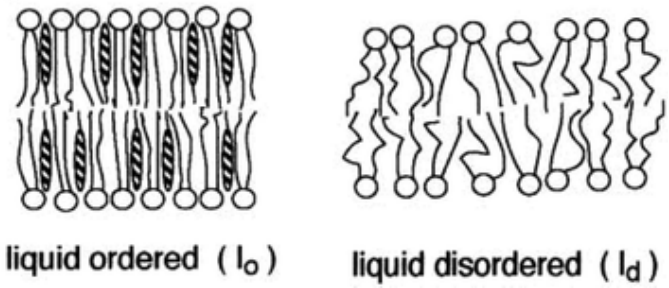

Figure 1.1: Illustration of liquid ordered phase and liquid disordered phase. From Furt et al., 2011.

Biophysical properties of lipids play important roles in the assembly of microdomains, with cholesterol interacting favorably with saturated lipids but with repulsion to unsaturated lipids, same with saturated and disordered lipids. Proteins are important for the organization of the microdomains and the cytoskeleton, more precisely microtubules, influencing density and size of microdomains in the PM (Szymanski et al., 2015; Yu et al., 2020).

While the microdomains of an animal cell are mobile, plant microdomains seem more immobile. This could be due to attachment of the PM to the cell wall (Szymanski et al., 2015). However, the microdomains are not completely static either since movement of microdomain marker proteins has been linked to microtubule depolymerization (Yu et al., 2020).

1.1.3 The cell wall integrity (CWI) maintenance mechanism

The cell wall can also be subjected to mechanical damage caused by wounding, environmental stress (e.g., by ice crystals formed during cold stress or ion toxicity leading to disruptions of the pectin structure) or herbivory, and pathogens can damage the cell wall using cell wall degrading enzymes (Lorrai & Ferrari, 2021; Novaković et al., 2018; Savatin et al., 2014).
While biotic stress often arises in a specific area of the plant, abiotic stress tends to be more systemic and impact large parts of the plant, exemplified by drought. Still, both can result in

cell wall damage (CWD), which impairs the functional integrity of the cell wall (Novaković et al., 2018).
Abiotic stress like drought and freezing have in common that they affect the water potential of the cell, which in turn affects the turgor pressure, an effect comparable to the effects osmotic stress has on the plant (Novaković et al., 2018).

In non-stress conditions, the cell has positive pressure potential (turgor pressure), which is contained when the PM presses against the cell wall. In hyper-osmotic conditions on the other hand, the cell will lose water to its surroundings, causing the PM to shrink and eventually lead to displacement from the cell wall, distorting the PM-cell wall continuum (Roumeli et al., 2020; Vaahtera et al., 2019). This is called plasmolysis. Last, in hypo-osmotic conditions the cell will gain more water due to osmosis, resulting in higher turgor pressure. The exertion of higher turgor pressure on the cell wall causes the cell to be more stiff than under normal or hypo-osmotic condition (Roumeli et al., 2020). If the cell wall is experiencing CWD, the prevalent high turgor pressure seems to push against the wall, causing PM stretch, cell deformation and additional damage (Gigli-Bisceglia et al., 2020; Vaahtera et al., 2019). This seems to be case based on results from work with the herbicide Isoxaben (ISX). This herbicide is often used to cause CWD in plants (Denness et al., 2011; Scheible et al., 2001). ISX, (N-3[1-ethyl-1-methylpropyl]-5-isoxazolyl-2,6, dimethoxybenzamide), blocks cellulose synthesis in actively elongating cells, leading to weakened cell walls and activation of stress responses (Engelsdorf et al., 2018; Scheible et al., 2001; Vaahtera et al., 2019). Downstream stress responses caused by ISX-induced CWD include accumulation of callose and lignin, production of phytohormones salicylic acid (SA), jasmonic acid (JA) and ethylene, generation of reactive oxygen species (ROS) and activation of Ca^{2+}-based signaling (Chaudhary et al., 2020; Engelsdorf et al., 2018; Hamann et al., 2009). Hyperosmotic stress, inducible with an osmoticums (such as sorbitol) on the other hand induce abscisic acid (ABA) production (Bacete et al., 2022). When seedlings are treated simultaneously with ISX and an osmoticum, i.e. CWD and reduced turgor pressure, the effects of ISX-treatment are suppressed in a concentration dependent manner (Hamann et al., 2009; Denness et al., 2011). This suggests that CWD-induced responses are activated by a turgor sensitive process (Engelsdorf et al., 2018; Vaahtera et al., 2019).

The cell wall integrity (CWI) maintenance mechanism makes it possible for the plant to adapt to biotic and abiotic stress, and it is also important during biological processes where the cell

wall actively remodels such as during growth and development (Bacete & Hamann, 2020). There are several stimuli that may activate the CWI maintenance mechanism, for instance Damage-Associated Molecular Patterns (DAMPs) derived from the cell wall, Pathogen-Associated Molecular Patterns (PAMPs), distortion of the PM itself or the displacement of the PM relative to the cell wall (Vaahtera et al., 2019). Plants can respond by releasing DAMPs after detecting PAMPs or cell damage (Gigli-Bisceglia & Testerink, 2021; Q. Li et al., 2020). PAMPs and DAMPs are recognized by pattern recognition receptors (PRRs) at the cell surface. PRRs include receptor-like proteins and receptor kinases (Q. Li et al., 2020; Zhou & Zhang, 2020). For instance, rapid alkalinization factors (RALFs) are considered DAMPs and are recognized by *Catharanthus roseus* RECEPTOR-LIKE KINASE1-LIKE family (*Cr*RLK1L) members (Ge et al., 2019).

Plants could sense osmotic stimuli (osmo-sensing) in different ways: hyper-osmotic stress could be sensed by shrinking of the plasma membrane, involving for example the membrane-localized ion channel REDUCED HYPEROSMOLALITY INDUCED CA2+ INCREASE 1 (OSCA1), responsible for hyperosmolality induced Ca^{2+} increase of cytosol (Haswell & Verslues, 2015; Yuan et al., 2014). Increased plasma membrane tension (caused by hypo-osmotic stress) could be detected by mechano-perception channels, such as MID1 COMPLEMENTING ACTIVITY 1 (MCA1) (Bacete & Hamann, 2020; Haswell & Verslues, 2015). MCA1 is a mechanosensitive Ca^{2+} channel that is involved in both mechano-perception and hypo-osmotic stress perception (Engelsdorf et al., 2018). Lastly, altered CWI, i.e. cell wall disruption or movements, could be detected by receptor-like kinases, capable of sensing these events, such as THESEUS1 (THE1) and FERONIA (FER), members of the *Cr*RLK1L family (Haswell & Verslues, 2015; Vaahtera et al., 2019). THE1 and FER are localized at the PM, have malectin domains on the extracellular side and kinase domains on the cytoplasmic side. The malectin domains of THE1 and FER possibly interact with the cell wall directly or indirectly (cell-wall-derived ligands) (Bacete & Hamann, 2020). Both have been shown to interact with RALFs, RALF34 with THE1 and RALF1 and RALF23 with FER (Gonneau et al., 2018). FER is important in salt stress resistance and mechano-perception in *Arabidopsis* roots, while THE1 is required for production of SA and jasmonic acid JA in response to CWD (Bacete & Hamann, 2020; Vaahtera et al., 2019). Recently published results also suggest that THE1 acts upstream of MCA1 in response to ISX-induced CWD (Engelsdorf et al., 2018). It has also been implied THE1 can modulate ABA production or acts as a negative regulator of ABA production in response to hyper-osmotic stress (Bacete et al., 2022). Sensors that can

sense hypo-osmotic and hyper-osmotic stress induced changes of the PM could give the cell essential information about the state of cell wall PM continuum, especially combined with information from other sensors as well (Vaahtera et al., 2019).

This simplified overview indicates there is evidence for a mechano-/turgor sensitive processes involving the PM and the cell wall that is responsible for activation of the CWD response., the mechanosensitive fluorophore Flipper-TR, described below, can hopefully help us find out more of what is happening with PM tension under osmotic stress.

1.2 Microscopy

1.2.1 Confocal laser scanning microscopy (CLSM)

The conventional microscope requires the sample to be thin, or at least cut into thin sections, which can be a problem if one wants to study living organisms with tissue thicker than about 10 μm (M. Shotton, 1989; Nwaneshiudu et al., 2012). The advantages of fluorescence microscopy such as use of green fluorescent protein (GFP) are in these cases diminished as the light emitted excites fluorescence throughout the whole sample, not just at the focal point. The objective lens will amass/accumulate fluorescence from the whole sample, causing blur in the collected image (Hepler & Gunning, 1998; M. Shotton, 1989). One solution to this problem is using a confocal laser scanning microscope when working with thicker tissue.

Marvin Minsky developed the confocal microscope in the 1950's, and by the late 1980's the CLSM was a widely used tool in biological research (Jonkman & Brown, 2015; Minsky, 1988). A widefield fluorescent microscope illuminates the entire sample at once, also parts outside the focal point of the objective lens, so there is background "noise" causing blurred images (Nwaneshiudu et al., 2012). In contrast, in a CLSM a laser beam is focused inside the sample with the help of the microscope objective. The fluorescent emission from the sample is then projected through a pinhole aperture and out-of-focus fluorescence is blocked (Jonkman & Brown, 2015; Nwaneshiudu et al., 2012), (figure 1.2). The light that hits the detector from one spot forms one pixel in the finished image. The focal point is moved so it scans the sample in a x-y plane, making an image of one plane of the sample (Nwaneshiudu et al., 2012). The focal plane can then also be moved along the z axis (depth) and additional xy planes can be imaged.

Using this approach it is possible to generate a 3D image of the fluorescent signals in the sample analyzed (Jonkman & Brown, 2015)

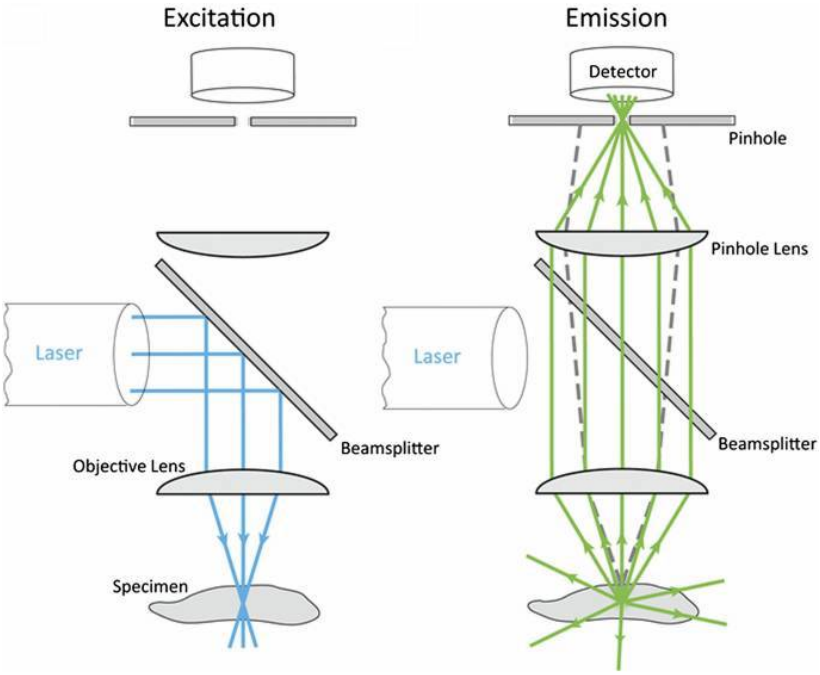

Figure 1.2: Schematic of a confocal light path. Source: Jonkman & Brown, 2015. (Originally form Methods in Cell Biology V123, p113-134, 2014.)

The invention and improvements of the CLSM have been important for fluorescence microscopy, as it is a great tool for e.g. cell biologists, neuroscientists and plant biologists. Today, different methodologies are used to quantify fluorescence in order to investigate protein-protein interactions and cellular dynamics. These include fluorescence resonance energy transfer (FRET), fluorescence recovery after photobleaching (FRAP), fluorescence correlation spectroscopy (FCS) and fluorescence lifetime imaging microscopy (FLIM) (Hamilton, 2009). In the context of this thesis FLIM will be employed.

1.2.2 FLIM

FLIM generates a spatial map of the lifetime(s) of the fluorophore(s) in a sample (Prasad, 2003). When a molecule, in the context of FLIM a fluorophore, absorbs the energy of light, electrons are excited to a higher energy level for a time, before going to the lowest vibrational level in the excited level by processes such as internal conversion and vibrational relaxation. The electrons return to the ground state in one of two ways, radiative or nonradiative process. In the radiative process a photon for each electron returning to the ground level is emitted,

which we can observed as fluorescence (Datta et al., 2020), see figure 1.3. The nonradiative process is when excitation energy dissipates by vibrational relaxation and collision quenching (excited fluorophore loses its energy when coming in contact with other atoms or molecules), which are thermal processes (So & Dong, 2001).

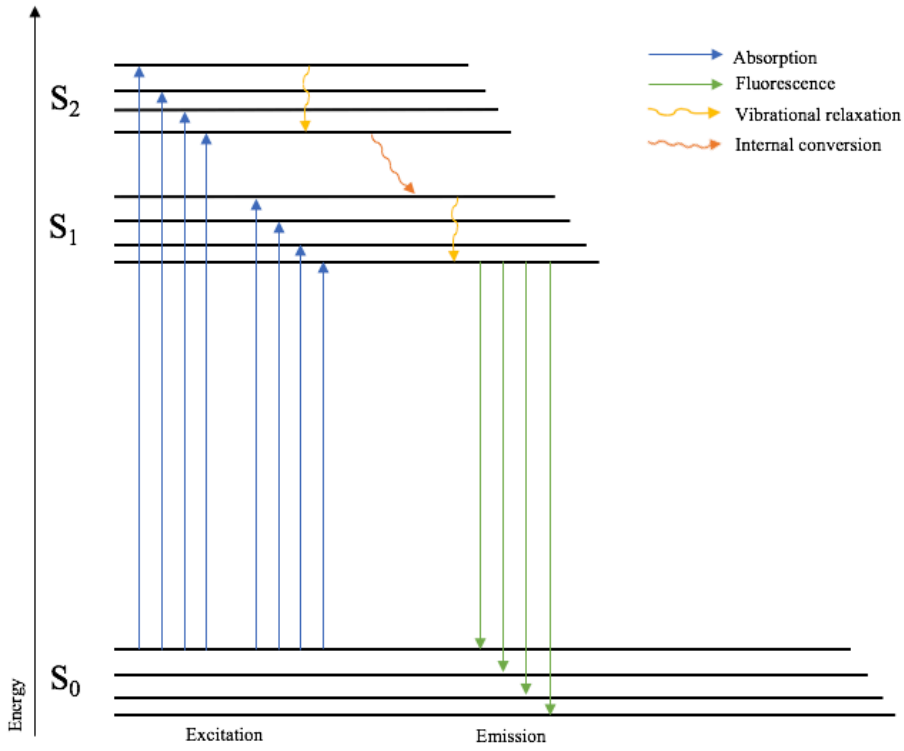

Figure 1.2: Jablonski diagram. Shows electron path after absorption of energy from photon.

The emitted energy is lower than the absorbed energy because of energy loss during internal conversion and vibrational relaxation. This causes the wavelength of the fluorescent emission to have a longer wavelength (Datta et al., 2020). The fluorescent lifetime is the time the electron is in the excited state before going back to ground state (Datta et al., 2021). The local environment (pH, temperature, ion concentration) of the fluorophore affects the fluorescent lifetime. Therefore, FLIM can be used to monitor these parameters (Datta et al., 2020). At the same time fluorescent lifetimes are independent of the fluorophore concentration, intensity and to some extent photobleaching (Prasad, 2003).

There are two ways of measuring lifetimes, time-domain or frequency-domain (X. F. Wang et al., 1992). I will focus on the time-domain here, as that is the method I have used.

With time-domain, a short pulse excites the fluorophore and then the fluorescence emitted is recorded as a function of time. Time-correlated single photon counting (TCSPC) is often used to do this (de Almeida et al., 2009). A single photon is recorded after a short light pulse and this is repeated until one ends up with a histogram of single photon counts, representing the decay curve, see figure 1.4 (Datta et al., 2020; de Almeida et al., 2009).

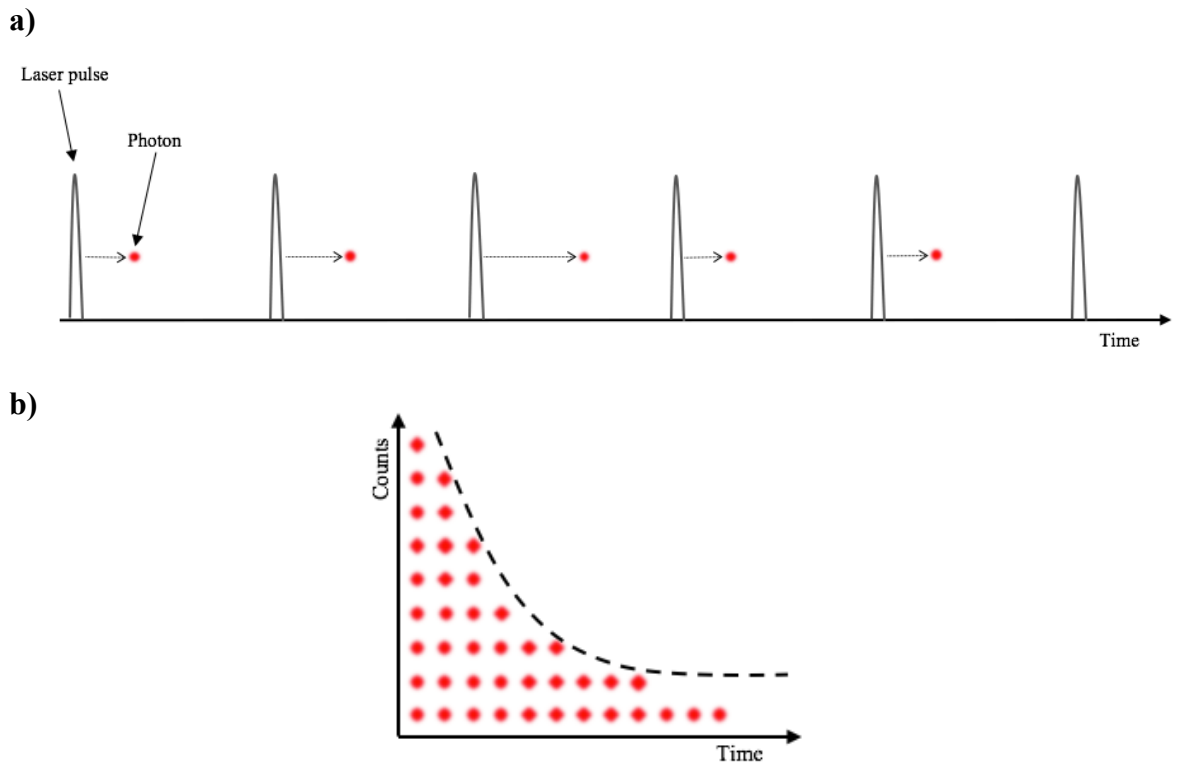

Figure 1.3: Time-correlated single photon counting**. a)** Principle of excitation by laser and recording of single photon, done repeatedly. **b)** TCSPC histogram.

TCSPC is a slower method compared to other FLIM techniques such as time gating (histogram from narrow time-gated detection of photons) or frequency-domain FLIM (Datta et al., 2020). This is because there have to be a low photon count after a pulse not to get a bias towards shorter lifetimes due to the instruments inability to record more photons when it is processing the first photon detected (instrument dead time) (Datta et al., 2020; Liu et al., 2019; van Munster & Gadella, 2005). An advantage of TCSPC on the other hand is the high accuracy of lifetime estimations (Datta et al., 2020).

A curve fitting analysis can be done with the TCSPC histogram to determine the estimated lifetime (Datta et al., 2020). For a single exponential decay:

$$I(t) = Ae^{-t/\tau} \quad (1\text{-}1)$$

Where I is intensity at t time, A is the amplitude of the exponential function (number of photons at t = 0 and τ is the lifetime, which is the time A of the fit curve decays to A/e. With double exponential decay the curve is biexponential, and two amplitudes and lifetimes can be calculated (Datta et al., 2020).

1.2.3 Flipper-TR

The fluorescent lipid tension reporter Flipper-TR (formerly FliptR) is a fluorophore that inserts into lipid membranes without disturbing membrane order. It consists of two dithienothiophene (DTT) groups (often called "flippers") connected with a rotatable bond, and a headgroup with a negatively charge carboxyl help the probe insert itself correctly ("oriented insertion") in the membrane. The twisting of the DDT groups is aided by methyls and endocyclic sulfurs next to the bond (Colom et al., 2018). See figure 1.5.

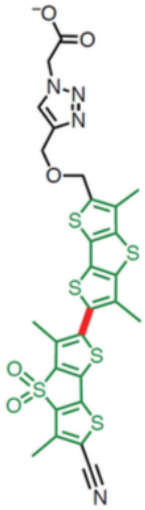

Figure 1.4: Chemical structure Flipper-TR. From Colom et al., 2018.

A push-pull probe such as Flipper-TR has an electron donor structure and electron acceptor structure (L. Li et al., 2020), which results in a negatively charged structure when the molecule is in certain conformations (Assies et al., 2021). The configuration of the push pull probe Flipper-TR is dependent on the lipid packing of the membrane, which in turn depends on and is affected by the tension of the lipid membrane. Lipid packing is the density of the acyl chains

of the membrane, with higher lipid packing corresponding with tighter and more ordered acyl chains whereas more spaced and disordered acyl chains correspond with lower lipid packing (Colom et al., 2018). In mixed membranes increased tension was found to cause increased lifetime while decreased tension caused decreased lifetime of the fluorophore. The increase in lifetime in cells upon increased tension comes mostly from membrane reorganization, which again is driven mainly from microdomain assembly (Assies et al., 2021). For decreasing tension other contributions, such as membrane curvature changes, rippling and rejection of excess lipid, become more important (Assies et al., 2021). The fluorescence lifetime of the probe in a membrane can be measured using fluorescence-lifetime imaging microscopy. When membrane tension changes, the configuration of the mechanophore also changes, resulting in a change of fluorescence lifetime. This way we can get an idea of membrane tension changes in living cells (Colom et al., 2018). An application of Flipper-TR is illustrated by the work of Roffay et al. (2021). The authors used Flipper-TR to study the relationship between cell volume and membrane tension in mammalian cells (HeLa cells). One thing they found was that coupling between cell volume and tension is kept for at least 20 minutes after an osmotic shock (Roffay et al., 2021). Figure 1.6 shows cell volume change and PM tension change after osmotic treatment (Roffay et al., 2021).

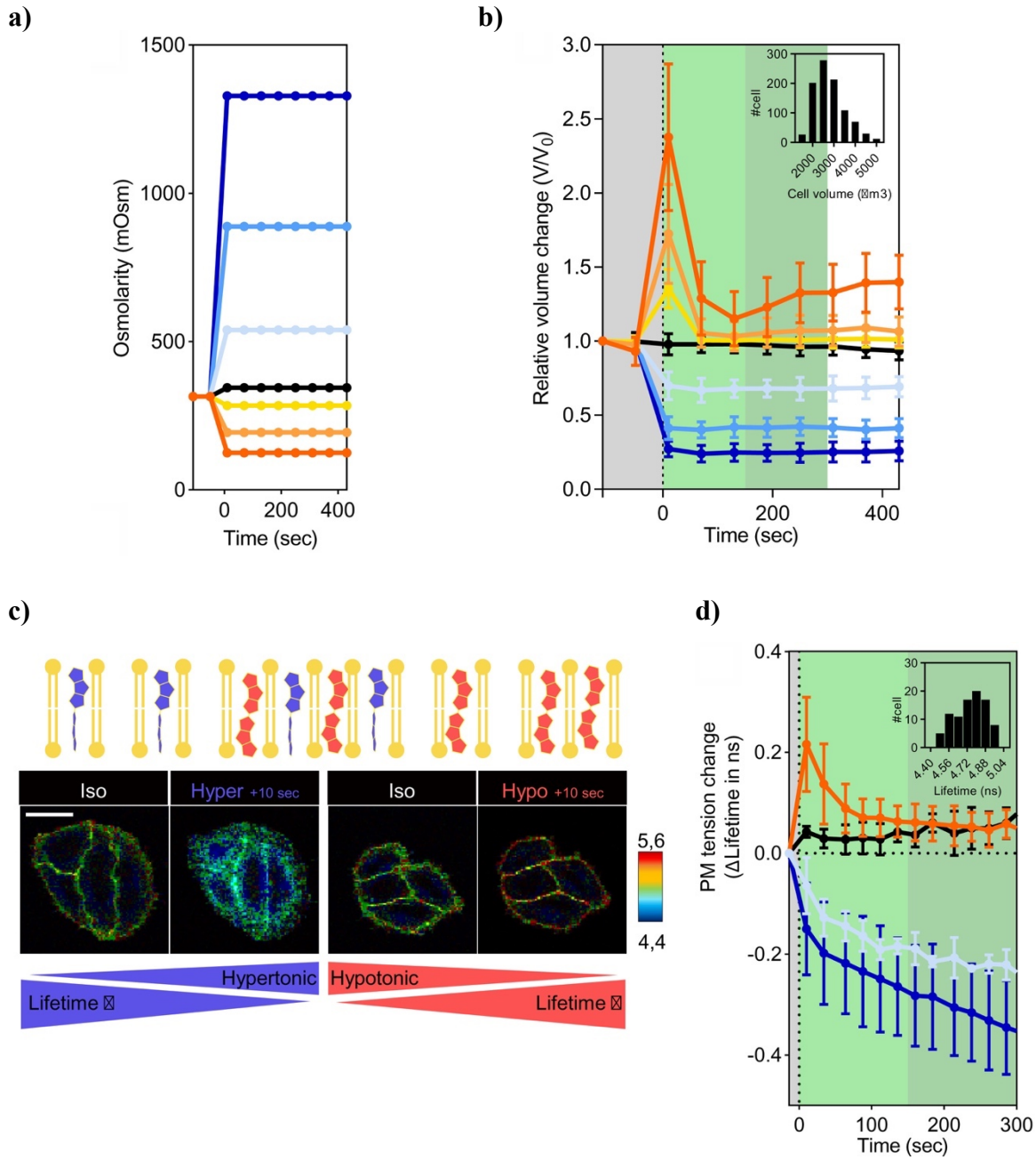

Figure 1.5: Cell volume and PM tension change after osmotic treatment. **a)** The osmolarities in mOsm of the cell media, where dark orange = 120 mOsm, light orange = 190 mOsm, yellow = 285 mOsm, blac = 315 mOsm, light blue = 540 mOSm, medium blue = 890 mOsm and dark blue = 1330 mOsm. Color code is maintained. **b)** Relative volume change under osmotic shock, where grey is before shock, light green is short term response and dark green is long term response**. c)** Flipper-TR lifetime values for different osmotic conditions, shown in colorscale. **d)** Changes in PM tension, measured using Flipper-TR, during osmotic treatments. Figure from Roffay et al., 2021.

Flipper-TR has also been used to study TORC2's (target of rapamycin complex 2) function in PM dynamics regulation (Assies et al., 2021). TORC2 was found to function as a negative

feedback loop to maintain the tension of the PM in the optimal window. With an increase or decrease in PM tension the TORC2 kinase activity increased or decreased, while inhibition of TORC2 was found to lead to increased PM tension and hyperactivation of downstream signaling of TORC2 lead to low membrane tension (Assies et al., 2021; Riggi et al., 2020). Figure 1.7 shows changes in PM tension via changes in Flipper-TR lifetime in response to (a) TORC2 inhibition and (b) elevated TORC2 signaling (Riggi et al., 2018).

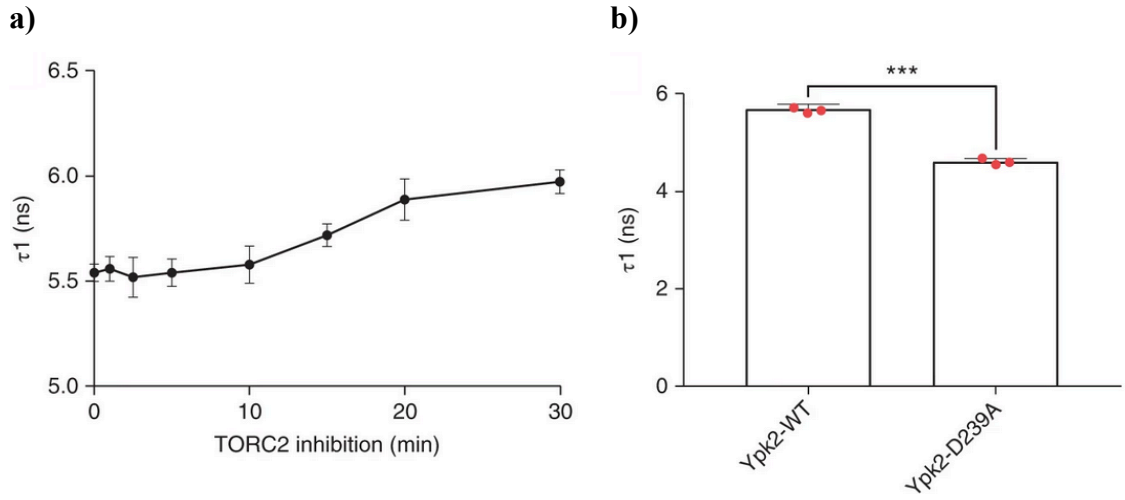

Figure 1.6: Changes in PM tension via changes in Flipper-TR lifetime.**a)** TORC2 inhibition by rapamycin in TOR1-1 AVO3Δ1274–1430 cells and mean lifetime (τ1) of Flipper-TR ± s.d. measured by FLIM, shows increased tension with TORC2 inhibition. **b)** Lifetime (τ1) of Flipper-TR measured by FLIM in wt and hyperactive version of YPK2 cells (***P < 0.001, two-tailed unpaired t-test, P = 0.00014), shows lower PM tension with elevated TORC2 signaling Figure from Riggi et al., 2018.

Flipper-TR was developed using giant unilamellar vesicles (GUVs), and for living cells: HeLa fibroblastic cells and MDCK epithelial cells (Colom et al., 2018). Several of the probes qualities makes it a good candidate for analysis of PM dynamics in living plants, including minimal fluorescence in water, partitioning comparably into different membrane domains and not disturbing the membrane structure it inserts into (Colom et al., 2018). However, no peer-reviewed publications exist describing the use of Flipper-TR in plants. Labeling has been successfully performed on root tips and leaves, but only as proof of principle (Cytoskeleton and Spirochrome, personal communication, April 29, and June 15, 2021).

1.3 Aim of thesis

The existing knowledge indicates that turgor pressure perception and mechano-sensing likely have important roles in the plant CWI maintenance mechanism. The relevant processes take probably place at the intersection between the PM and the cell wall. Therefore, it would be interesting to understand how membrane tension in changes when the cell wall and plasma membrane are disturbed/compromised and to compare the state of the membrane under "normal" conditions with different stress conditions (ISX-treatment, sorbitol-treatment and ISX + sorbitol co-treatment).

Therefore, the aims of this thesis are to examine if Flipper-TR can be used to investigate membrane tension and organization in plants and if that is the case, use it to characterize the effects CWD and turgor manipulation have on membrane tension and organization. First, the staining method has to be adapted for use in *Arabidopsis* seedlings, as it was developed for use in animal cells. Then I will use Flipper-TR to investigate PM tension in plant root cells in normal vs. stress condition using FLIM, in order to establish these cells as model system to investigate changes in plasma membrane tension.

2. Materials & methods

All chemical reagents and labware were bought from Sigma Aldrich (Merck) unless otherwise specified.

2.1.1 Plant material

Arabidopsis thaliana ecotype Columbia 0 (Col-0) was available from Hamann lab. Wave 131Y (Columbia background) was generated by the Geldner lab at the University of Lausanne and acquired from the Nottingham Arabidopsis Stock Center.

2.2 Seed sterilization and plant growth

2.2.1 Sterilization of seeds

Seeds were sterilized in Eppendorf tubes, by adding 500 µL 70% EtOH, rotating for 5 minutes in a rotator (PTR-25 Mini Rotator, Grant Bio). The ethanol was discarded, then 500 µL 50 % bleach (Klorin, Lilleborg) was added, the seeds then rotated for 10 minutes. The bleach was discarded, and the seeds were washed three times with 500 µL MilliQ water.

2.2.2 Growing seeds in liquid media

Seeds were grown in multi-well plates (24 wells). 1 ml sterilized ½ Murashige and Skoog (MS) growth media (2.2 g/L MS basal media, 0.5 g/L MES salt, 1% sucrose, adjusted to pH 5.7 with HCl) and one seed was put in each well. The plate was closed and secured with surgical tape (3M™ Micropore™) to allow ventilation. The seeds were then stratified at 4˚C for two days. Plates were placed for 6 days in a growth chamber (Percival AR-66L2, CLF Plant Climatics) at 16 h daylight at 22 °C 150 µmol m^{-2} s^{-1} light intensity / 8 h dark at 18˚C on a IKA KS501 flask shaker at 130 rotations per minute.

2.2.3 Growing seeds on plates

About 20 seeds were placed in two rows on an ½ MS agar plate (2.2 g/L MS basal media, 0.5 g/L MES salt, 1% sucrose, adjusted to pH 5.7 with HCl, then put in 1% agar). The lid was secured with tape. The seedlings were stratified for two days at 4 ˚C, then were grown for 6 days in a growth chamber at 16 h daylight at 22 °C 150 µmol m^{-2} s^{-1} light intensity / 8 h dark

at 18˚C After 5 days the seedlings were transferred to a multi well plate (6 wells) with sterilized ½ MS liquid media and placed on a flask shaker at 130 rotations per minute.

2.3 Time course experiment with Wave 131Y seedlings

Wave 131Y seeds were sterilized and grown in liquid ½ MS media as described above Seedlings were first stressed in treatment solution in a 6-well plate for the right amount of time before being put on a microscope slide (VWR) with 70 µL propidium iodide (PI). The treatment solutions were either sorbitol (300 mM, 0.1% dimethyl sulfoxide (DMSO)), ISX (600 nM in DMSO), mock (0.1 % DMSO), ISX + sorbitol (600 nM ISX in DMSO, 300 mM sorbitol) or phosphate buffered saline (PBS) (0.01 M, pH = 7.2).
The seedlings were covered with a no.1 coverslip (130-170 µm) (VWR) and then imaged using a Leica TCS SP8 CLSM with a 40x objective (1.10, water immersion). Pictures were taken at timepoints 1, 2, 3, 4, 5, 6 and 7 hours. Visible laser with excitations at 488 nm (GFP) or 552 nm (PI) were used, and emissions collected between 512-554 nm and 597-639 nm. Formats were 512x512 pixels, 400 Hz speed and pin hole was 1 airy unit.
Image processing was done using ImageJ.

2.4 Fluorescence lifetime imaging microscopy

2.4.1 Treatment of seedlings

Seedlings were stained in 200 µL Flipper-TR (Spirochrome) staining solution (concentration: 20 µM dissolved in ≥ 99.9 % anhydrous DMSO, in ½ MS) in an Eppendorf tube for one hour.

Seedlings were removed from the staining solution and dabbed dry on paper before being transferred to a well in a 6 well plate containing ½ MS media with either sorbitol (300 mM, 0.1% DMSO), ISX (600 nM, 0.1% DMSO), mock (0.1 % DMSO) or ISX + sorbitol (600 nM ISX, 0.1% DMSO, 300 mM sorbitol). The seedlings were stressed for 0h/5min, 60 min, 90 min, 120 min and 180 min before being characterized. Seedlings in ISX and mock were in addition to this also stressed for 4, 5, 6, 7 and 8 hours before imaging/measuring.

2.4.2 FLIM measurements

3 stained and treated seedlings were put on a microscope slide (VWR) with 70 µL corresponding sorbitol, ISX, sorbitol + ISX or mock solution, and covered with a no.1 coverslip (VWR).

For FLIM analysis a Leica TCS SP8 confocal microscope with TCSPC system PicoHarp 300 and single photon avalanche diode (SPAD) detector was used.

A 25x objective (0.95, water immersion) was used. The sample was mounted on the microscope and an area that looked representative of the *Arabidopsis* seedling root elongation zone was chosen with a focus on the epidermis. A pulsed White Light Laser (WLL) with an acoustic optical beam splitter (AOBS) at frequency 40 MHz with excitation at 488 nm and a 488 nm notch filter was used for excitation. For acquisition the parameters were: 512x512 pixel format, 200 Hz speed and pin hole set to 1 airy unit, with SPAD1-detector (565 - 610 nm). FLIM data were collected until sufficient number of photons were detected (>>1000).

2.4.3 FLIM analysis

The FLIM analysis was done with software PicoQuant SymPhoTime64. A region of interest (ROI) was chosen so that it included mostly cell membrane and involved at least around 1000 counts/photons. See figure xx for example.
A 2-exponential tailfit was performed on the TCSPC decay curve of the ROI.

$$y(t) = \sum_{i=0}^{2-1} A[i] \exp\left(-\frac{t-t_0}{\tau[i]}\right) + Bkgr_{Dec} \quad (2\text{-}1)$$

Where A is the amplitude of the n-th exponential, τ is the lifetime(s) of the fluorophore (Flipper-TR in this case), $Bkgr_{Dec}$ is the correction for decay background, and t_0 is the extrapolated reference point for scaling the amplitudes.

In order to find τ_1 the SymPhoTime64 software provides the option to first do an "initial fit", which starts the fit and establishes initial parameters using Monte Carlo searches. Then the option "fit" is used to perform a tailfit to optimize the fitting parameters for the TCSPC curve of the ROI, using maximum likelihood estimation (MLE). See figure 2.1 for an example of ROI. $\chi 2$ was checked to ensure the fit was good. $\chi 2 = 1$ is a good fit. It is unusual to get exactly 1, but the closer to 1 the better. See figure 2.2 for an example of how this could look.

a) **b)**

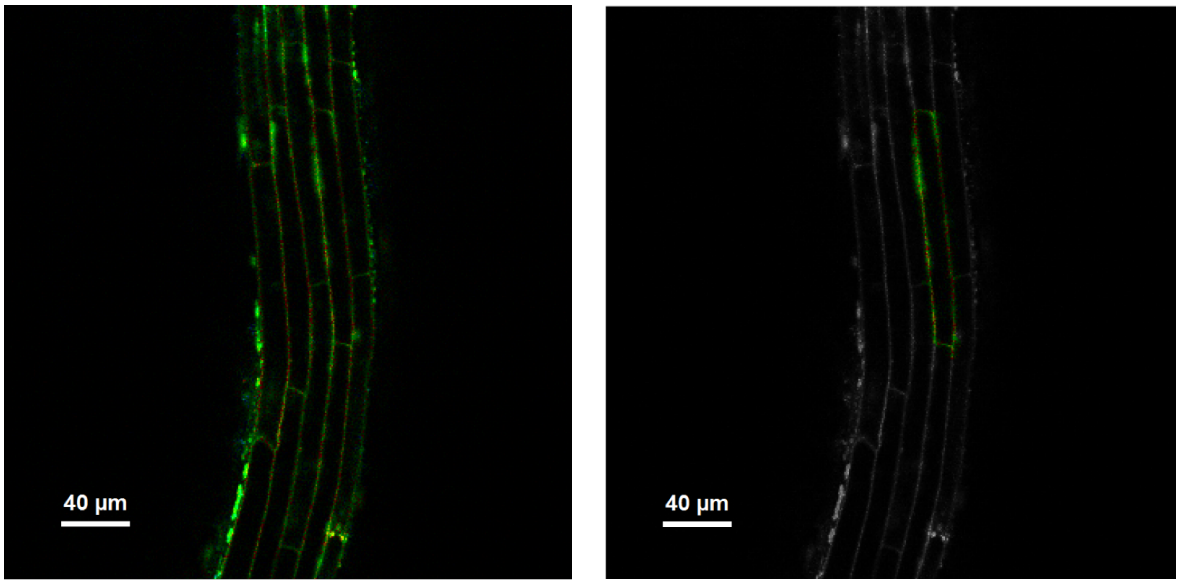

Figure 2.1: Choosing a ROI. **a)** Picture of Arabidopsis elongation zone in root stained with Flipper-TR. **b)** The green colored membrane is part of what the final ROI will be but does not include enough counts (photons) on its own.

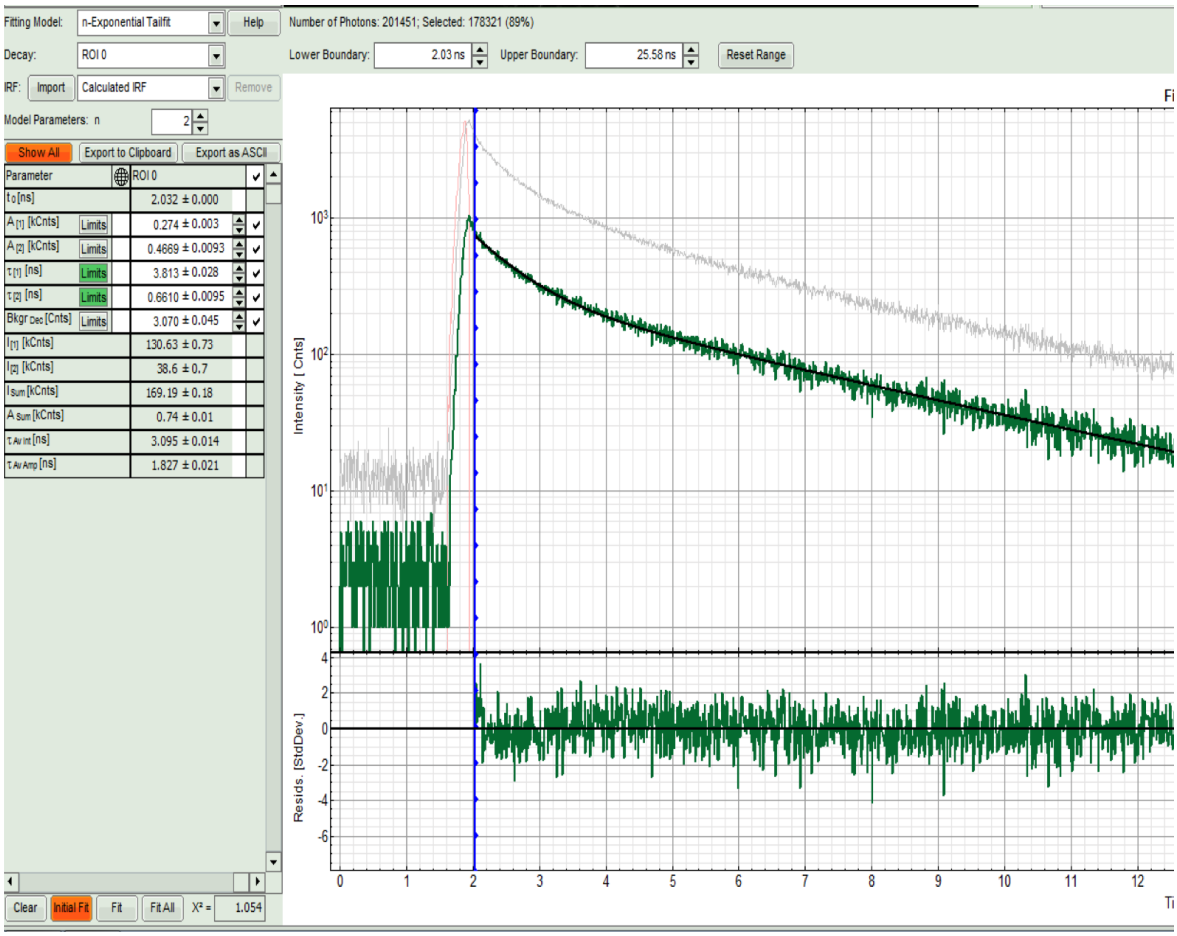

Figure 2.2: SymPhoTime64 user interface**.** Picture of an example decay curve being fitted in the SymPhoTime64 software. 2-exponential tailfit for ROI 1 is chosen where the top green line is ROI 1,

the black line is the fitted curve, $\boldsymbol{\tau}_1 = 3.813 \pm 0.028$ and $\chi 2 = 1.054$. An "initial fit" button (orange) and "fit" button is below parameters and values and beside the $\chi 2$-value. Residuals (bottom right) show no clear trend.

2.4.4 Data analysis

The violin plot and a line graph were made of the lifetime data using R and RStudio with ggplot2 and ggsci (R Core Team, 2020; RStudio Team, 2019; Nan Xiao, 2018; Wickham, H., 2016). Lifetimes at different timepoint for each treatment and lifetimes for the different treatments at the same timepoint were compared. A one-way ANOVA and Tukey Honestly Significant Difference (HSD) post hoc test ($\alpha = 0.05$), was calculated using RStudio (RStudio Team, 2019).

2.5 Validation of Flipper-TR and characterization of spectral properties of Flipper-TR using human cells

2.5.1 Preparation of material

HaCaT keratinocyte cells were provided by Felicity Ashcroft. The cells are maintained in Dulbecco's modified Eagle Medium (DMEM) supplemented with 5% (*v*/*v*) fetal bovine serum (FBS), 0.3 mg/mL glutamine, and 0.1 mg/mL gentamicin at 37 °C with 5% CO_2 in a humidified atmosphere.

HaCaT cells were seeded on 35 mm dishes with #1.5 coverslip bottoms (MatTek) 1 day before use. The media was removed and replaced with Flipper-TR staining media (2 μM Flipper-TR in DMEM supplemented with 0.3 mg/mL glutamine and 0.1 mg/mL gentamicin). The cells were stained for 15 min in 37 ˚C, humid environment.

2.5.2 Excitation and emission spectra

A Leica TCS SP8 confocal microscope together with the Leica Application Suite X (LAS X) were used for excitation and emission spectra. The spectra was obtained doing a Λλ- scan using the Excitation Emission Contour Plot. A 63x objective (oil immersion) was used, with (xyΛλ) scan parameters; λ_{ex} 470 – 565 nm, λ_{em} 480 – 700 nm using a WLL, with 5 nm excitation step

size and 20 steps, 19 nm detection step size and 11 steps, and a detection bandwidth of 30 nm. Pixel format was 256x256.

A picture of the area used for the excitation emission spectra was taken using WLL at 488 nm. Emission between 499 - 633 nm was collected. The format was 1024x1024 pixels, 400 Hz speed and pin hole was 1 airy unit.

Line graph showing excitation and emission maximum was made using RStudio (RStudio Team, 2019).

3. Results

Before using Flipper-TR to measure lifetimes in seedlings, the probe was validated in mammalian cells, measuring the fluorescence spectra of the probe. Then, experimental conditions were optimized using *Arabidopsis* seedlings. Subsequently the lifetime of *Arabidopsis* wild-type seedlings exposed to different osmotic conditions and ISX was measured at several timepoints to investigate if plasma membrane tension changes. The epidermal cells above the transition zone and below the initiation of the first root hair were used for the investigation as this is a region where cells start to expand, are therefore affected by ISX and expression of important cell wall integrity regulators is increased (Bacete et al., 2022).

3.1 Validation of Flipper-TR, Characterization of spectral properties and testing of experimental conditions

3.1.1 Excitation and emission spectra

The area used to measure the spectra in HaCaT keratinocyte cells stained with Flipper-TR can be seen in figure 3.1a, b. The spectrum obtained from cells stained with Flipper-TR was analyzed using a Λλ- scan, creating a λ^2-map (figure 3.1c). This map shows the fluorescence intensity at different excitation and emission wavelengths allowing detection of excitation and emission maximums. A plot was created using raw data from the Λλ-scan (figure 3.1d) (Appendix 1: table A.1). The spectra shows that Flipper-TR has an excitation maximum around 488 nm and emission maximum between 575-625 nm, which is consistent with the specifications in the Flipper-TR datasheet (Spirochrome, 2018). This shows that the spectral properties of Flipper-TR behave as expected in HaCaT cells.

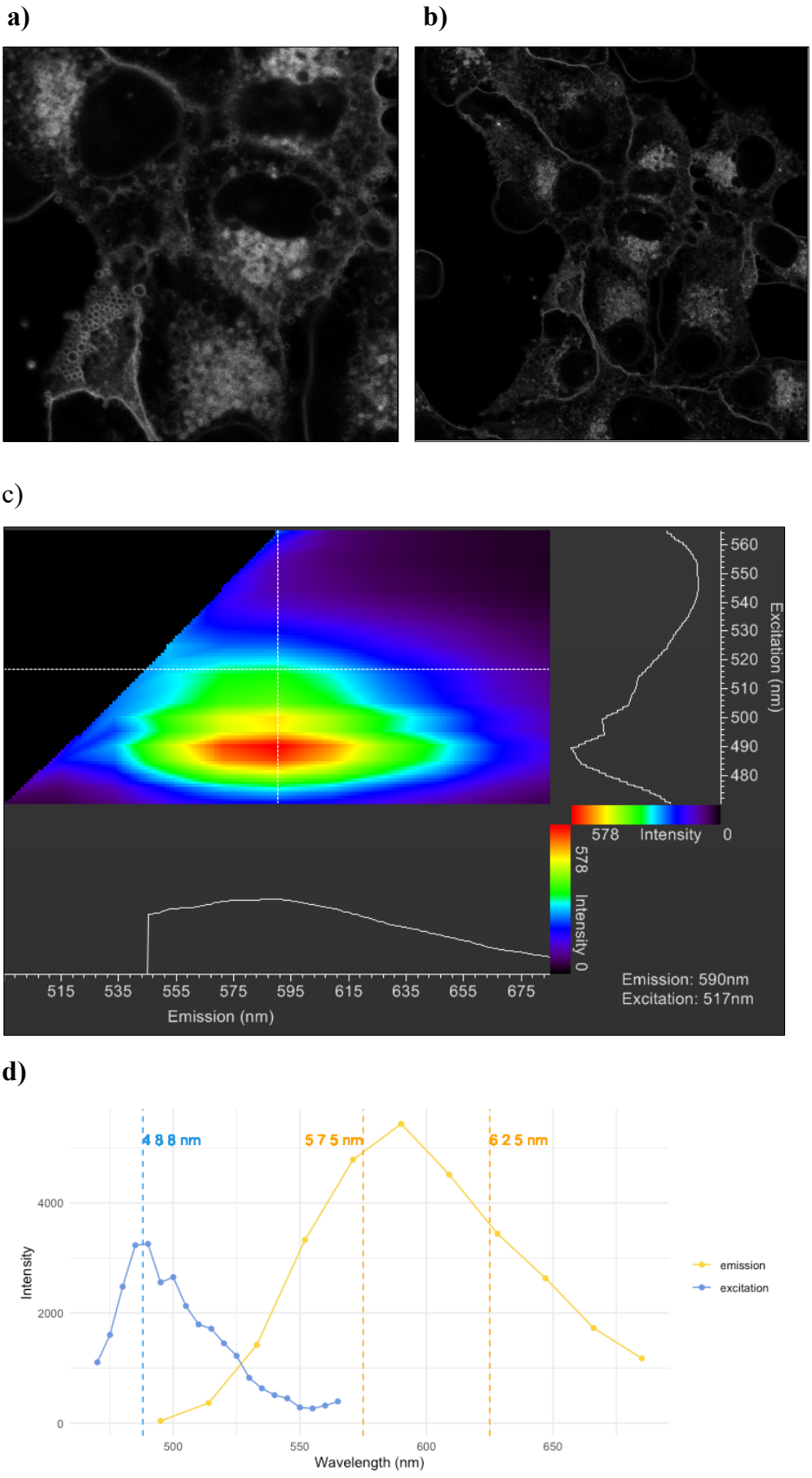

Figure 3.1: HaCaT cells stained with Flipper-TR and making an excitation and emission spectra. **a)** Area used to record excitation and emission spectra. **b)** Extended area surrounding the area where the spectra was recorded. **c)** λ^2-map. a 2-dimensional plot showing fluorescence intensity over excitation and emission

wavelength (nm), where red indicates the highest intensity and purple the lowest intensity. **d)** Plot showing peak excitation and emission wavelength, where x-axis indicates the wavelength and y-axis intensity. Excitation peak is around 488 nm and emission peak is around 600 nm.

3.1.2 PBS vs. ½ MS as solvent

With mammalian cells, cell media was used as solvent, but when the developers of Flipper-TR stained root tips and leaves as proof of concept, they used PBS (Cytoskeleton, personal correspondence, April 29, 2021). Here it was tested if PBS is suited as solvent when staining and treating seedlings. 6 days old Wave 131Y seedlings, expressing a fluorescent YFP (yellow fluorescent protein) marker located at the plasma membrane of cells, were treated with PBS or ½ MS (mock solution) for 2 hours and stained with PI (dye used for staining cell walls and assessing cell viability) (figure 3.2). PI and YFP signal were visible inside the cells treated with PBS. In comparison, seedlings treated with ½ MS only had staining of the cell borders. As PBS seems to be detrimental to the *Arabidopsis* root, possibly inducing cell death, ½ MS was chosen as solvent for the Flipper-TR stock solution and the different treatments, as it seems to have no detrimental effect on the seedling root.

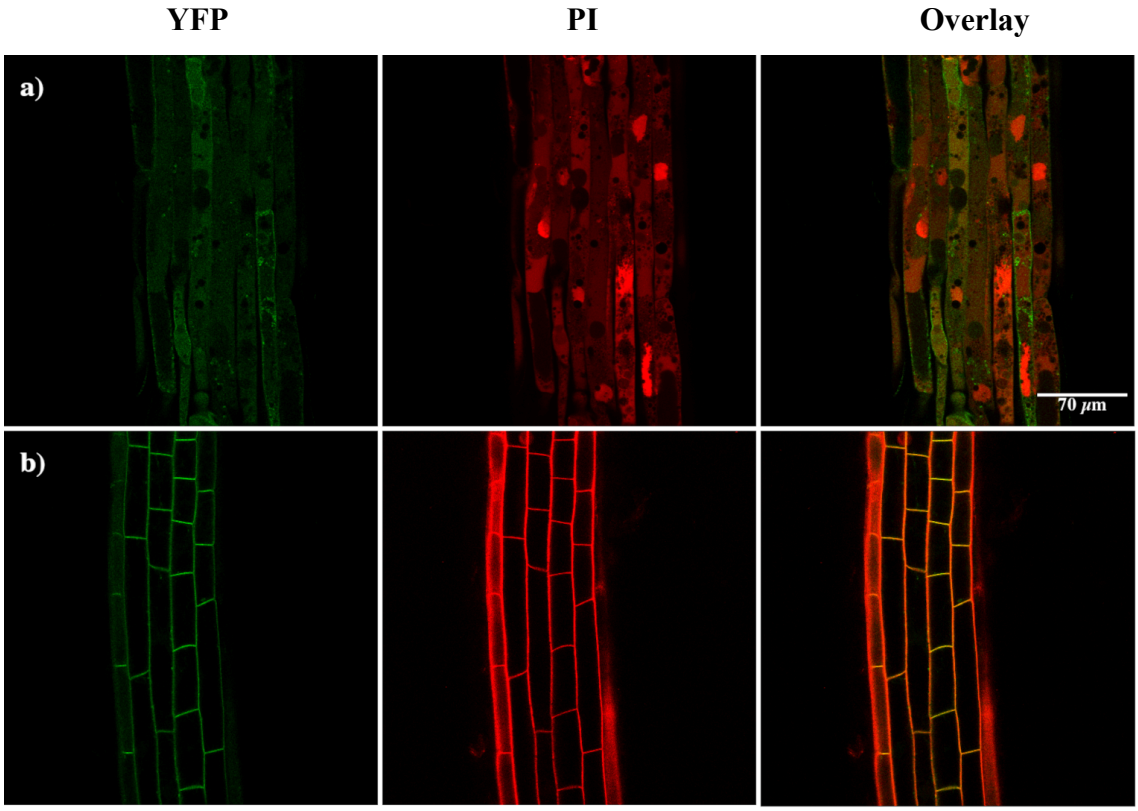

Figure 3.2: Wave 131Y seedling roots stained with PI. **a)** Wave 131Y seedlings treated with PBS for 2 hours before being stained with PI. **b)** Wave 131Y seedlings treated with mock solution (1/2 MS with 0.1 % DMSO) for 2 hours before being stained with PI.

3.1.3 Concentration of DMSO in the staining solution

To obtain a sufficient photon count (number of recorded photons in ROI) when doing FLIM, 20 µM Flipper-TR staining solution was used. Flipper-TR needs to be dissolved in ≥ 99.9 % anhydrous DMSO to make a 1 mM stock solution, this means the final staining solution contains ~2% (*v*/*v*) DMSO. A solution containing 2% DMSO in ½ MS was made to see the effects this concentration of DMSO has on the root cells after 1 hour, the amount of time seedlings are stained. Differences were detectable between seedling roots, which had been treated in this manner. Representative examples are shown in figure 3. Roots had either the majority of the cells not stained with PI or YFP signal inside the cell (Figure 3.3 a) or displayed cells with PI staining and YFP signal visible inside the majority of the cells (Figure 3.3 b). It seems 2% (*v*/*v*) DMSO likely has a negative effect on the cells, possibly inducing cell death, but this is not happening in all cells or all roots similarly.

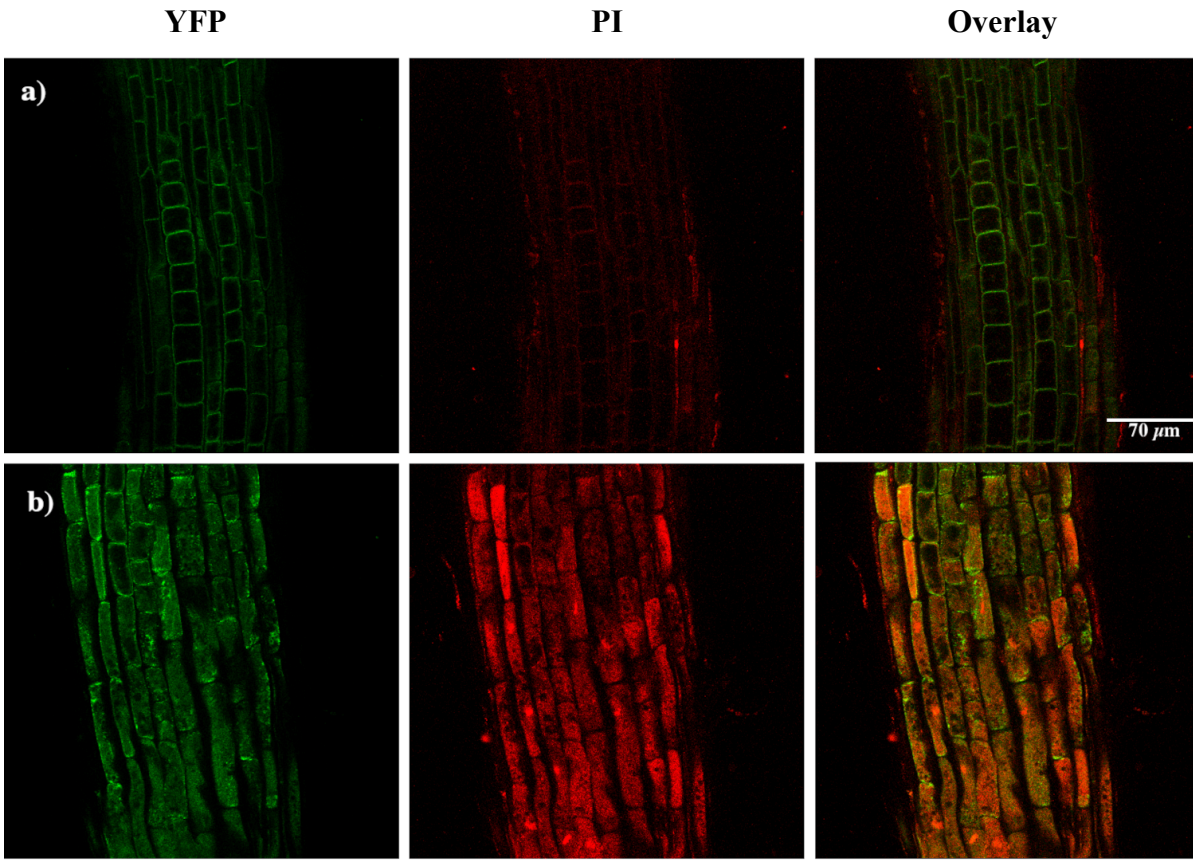

Figure 3.3: Wave 131Y seedlings treated with DMSO. **a)** Roots where fluorescence was only observed at the cell outline **b)** Roots where the fluorescence penetrated inside the cells.

3.1.4 Flipper-TR stains epidermal cells

Using the staining conditions established, seedling roots were stained with Flipper-TR and imaged using a confocal microscope. Figure 3.4 shows a representative picture, where the focal plane of the microscope was on a cell layer below the epidermis. There is no visible signal in the inner tissues, but the epidermis cells and root hairs at the sides are visible. Therefore, all FLIM measurements were done with the PMs of epidermal cells.

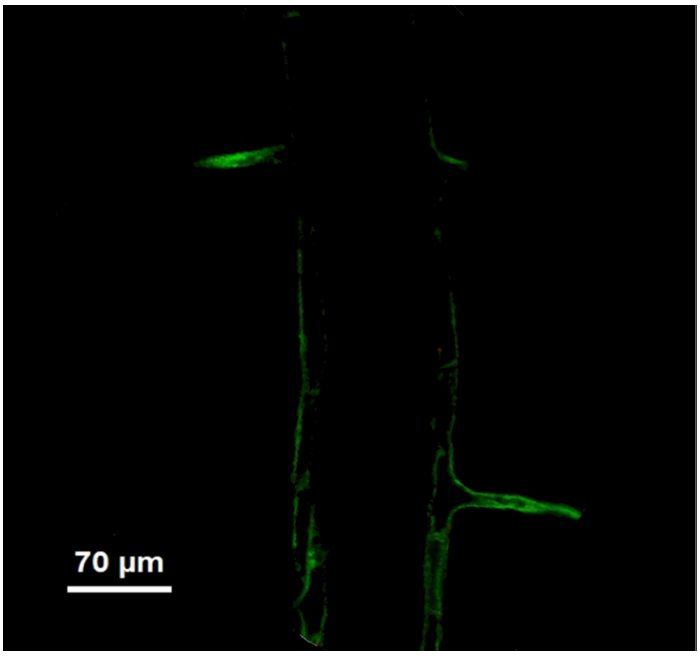

Figure 3.4: Col-0 root stained with Flipper-TR. The picture was obtained using a Leica SP8 and SymPhoTime64 with excitation at 488 nm.

3.1.5 Experimental troubleshooting

There was a contamination issue affecting the seedlings grown in tissue culture conditions. After first detecting the contamination a series of measures were taken, e.g., changing the sterilization solutions and changed from liquid to solid media. When this did not completely solve the issue, I did the measurements and took pictures in seedlings/root areas that did not seem affected.

3.2 Treatment effects on root cell shape

Initially the impact of changes in turgor and CWI on cell shape were assessed. Sorbitol, normally used to mimic drought-like conditions, was employed to manipulate turgor. ISX was used as a tool to cause CWD, weakening the cell wall and allowing expansion, caused by turgor. Six days old Wave 131Y seedlings were treated with mock, ISX, sorbitol or ISX +

sorbitol solution and imaged using a Leica SP8. To visualize the treatment effects the PM was labelled with YFP and the cell wall stained with PI.

3.2.1 Mock-treatment

Seedlings treated with mock solution were imaged at timepoints 1, 3, 5, and 7 hours. Cell walls and PMs look intact, with the fluorescent signals only visible outlining the cells (figure 3.5). The shapes of the cell wall and PM look similar in all seedlings. This suggests that the mock-treatment does not affect the seedling over time in a noticeable way.

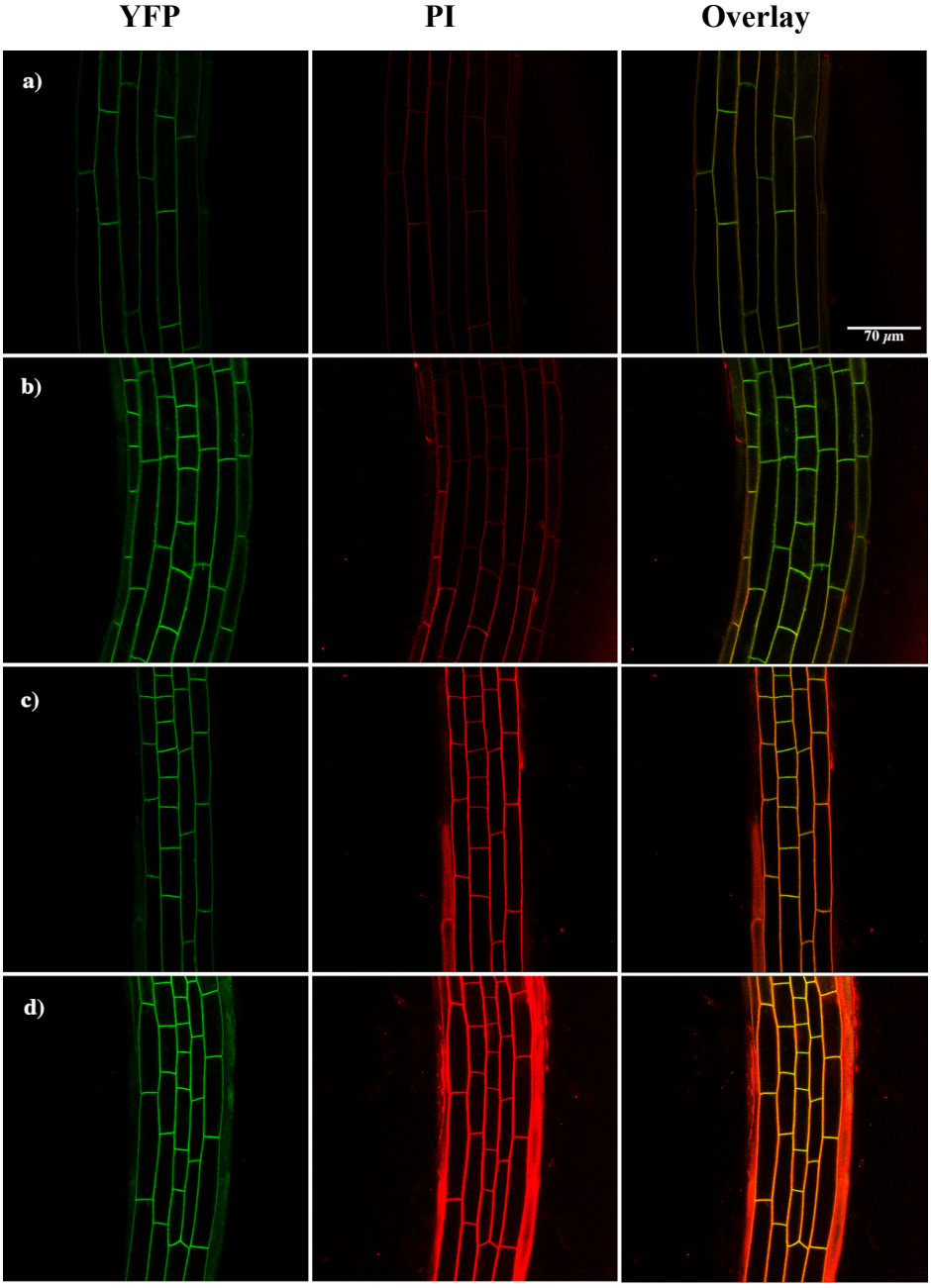

Figure 3.5: Mock-treated Wave 131Y seedlings stained with PI. The seedlings were treated with mock solution for **a)** 1 hour. **b)** 3 hours. **c)** 5 hours and **d)** 7 hours.

3.2.2 Sorbitol-treatment

Seedlings treated with sorbitol solution were imaged at timepoints 1, 2 and 3 hours because previous work has shown that ABA production is induced after 3 hours. This implies that perception of and response to sorbitol-treatment is induced before. After 1 hour seedlings looked similar to mock-treated seedlings (figure 3.6 a). For the 2 hours timepoint the YFP signal resembles the signal observed upon mock-treatments. However, the PI staining seems to stain more than just the cell wall surrounding the cell. This may indicate cell wall PM disruption and/or the beginning of cell death (figure 3.6 b). At the 3 hours timepoint it seems the PI stain has penetrated into some of the cells and is also more pronounced in spots or bands surrounding the rest of the cells (figure 3.6 c). This indicates the sorbitol-treatment has a detrimental effect on the root cells, which is getting more pronounced over time.

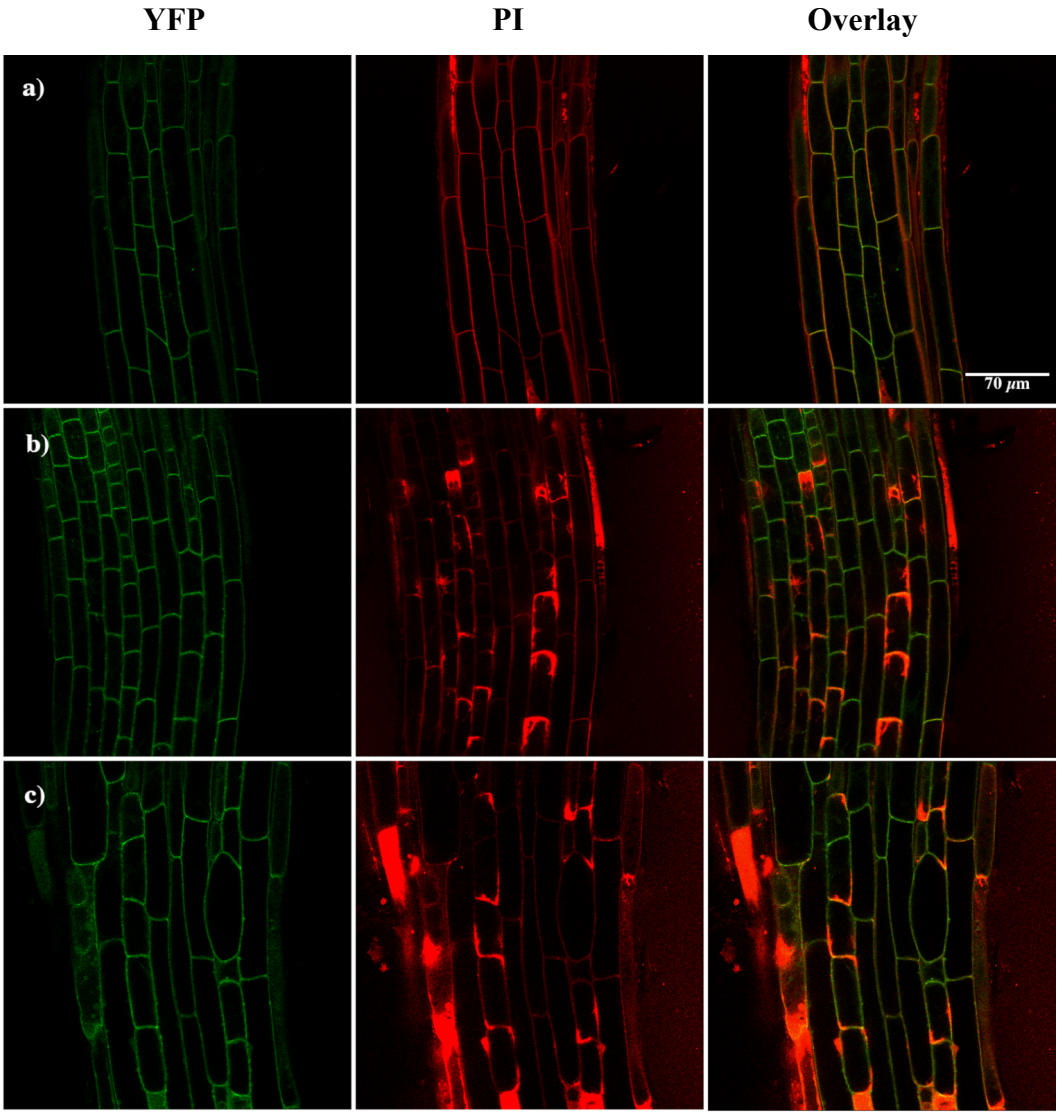

Figure 3.6: Sorbitol-treated Wave 131Y seedlings stained with PI. Seedlings that have been treated with a sorbitol solution for **a)** 1 hour. **b)** 2 hours and **c)** 3 hours.

3.2.3 ISX-treatment

Seedlings treated with ISX were imaged at timepoints 4, 5, 6 and 7 hours because morphological effects had been described before at these time points (Hamann et al., 2009). Cells look similar to mock at the 4 hours timepoint, with maybe the beginning of swelling, i.e., the radial growth compared to the length of the cell (figure 3.7 a). At 5 hours several cells exhibit different cell shapes than cells mock-treated, cells are swelling laterally and get overall a rounder shape /figure 3.7.b). This swelling is even more pronounced after 6 and 7 hours, and there is also staining of cell insides to different extents, suggesting cell death (figure 3.7 c & d). Cell swelling becomes more pronounced as time goes by and the inhibition of cellulose biosynthesis results in weaker cell walls.

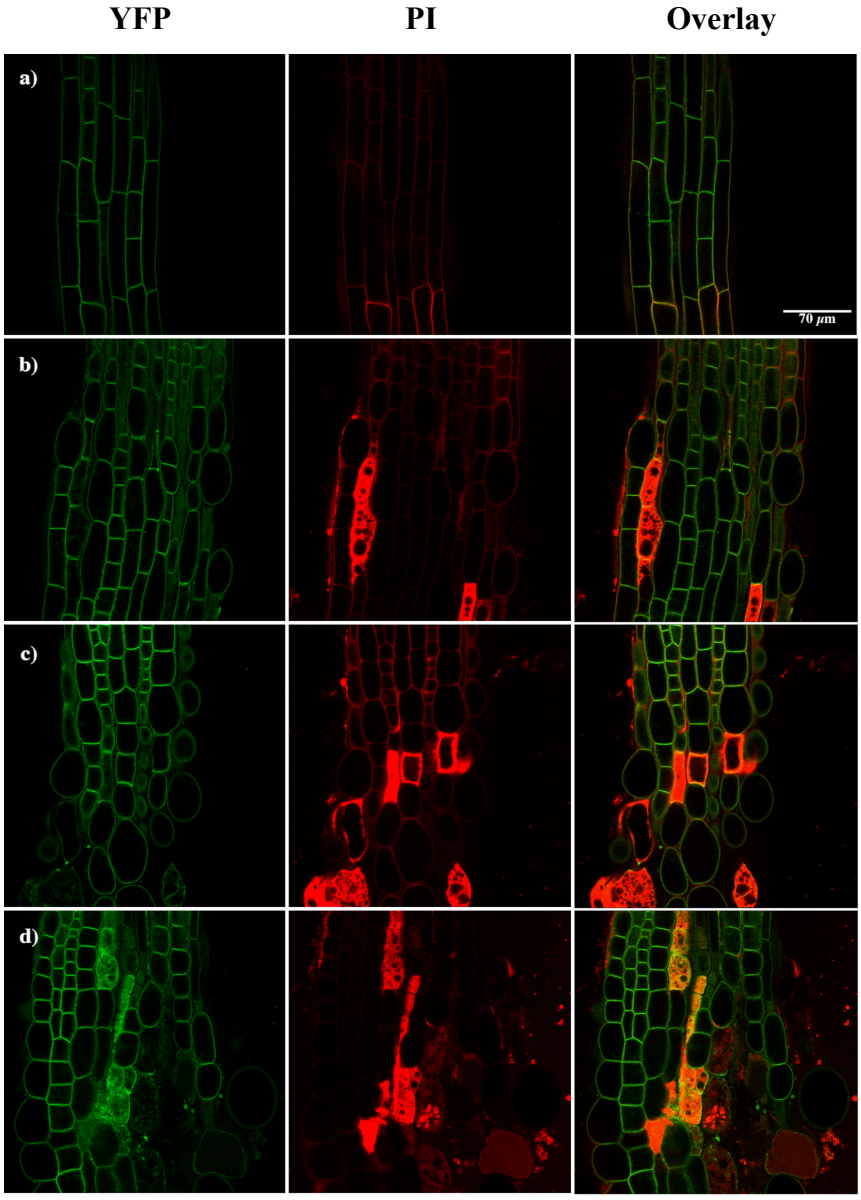

Figure 3.7: ISX-treated Wave 131Y seedlings stained with PI. Seedlings have been treated with ISX for **a)** 4 hours, **b)** 5 hours, **c)** 6 hours or **d)** 7 hours.

3.2.4 ISX + sorbitol-treatment

Seedlings treated with ISX + sorbitol were imaged at timepoints 3, 5 and 7 hours, since they cover the period where effects are observed with sorbitol and ISX individual treatments (figure 3.8). At the 3 hours treatment the cells resemble the cells from the mock-treatment but with a little PI staining. At the 5 hours timepoint cells exhibit some swelling compared to the mock condition cells, and with many cells being stained completely by PI. At the 7 hours timepoint cells seem to be more swollen, with several looking circular and pronounced PI staining. Interestingly, there are also cases where the PM seems still intact despite pronounced PI staining. Adding sorbitol to ISX seems to result in less pronounced cell swelling than just the ISX-treatment did, indicating sorbitol may dampen some of the effect. On the other hand, there appears to be more cell death, meaning the cells are not necessarily in a better condition.

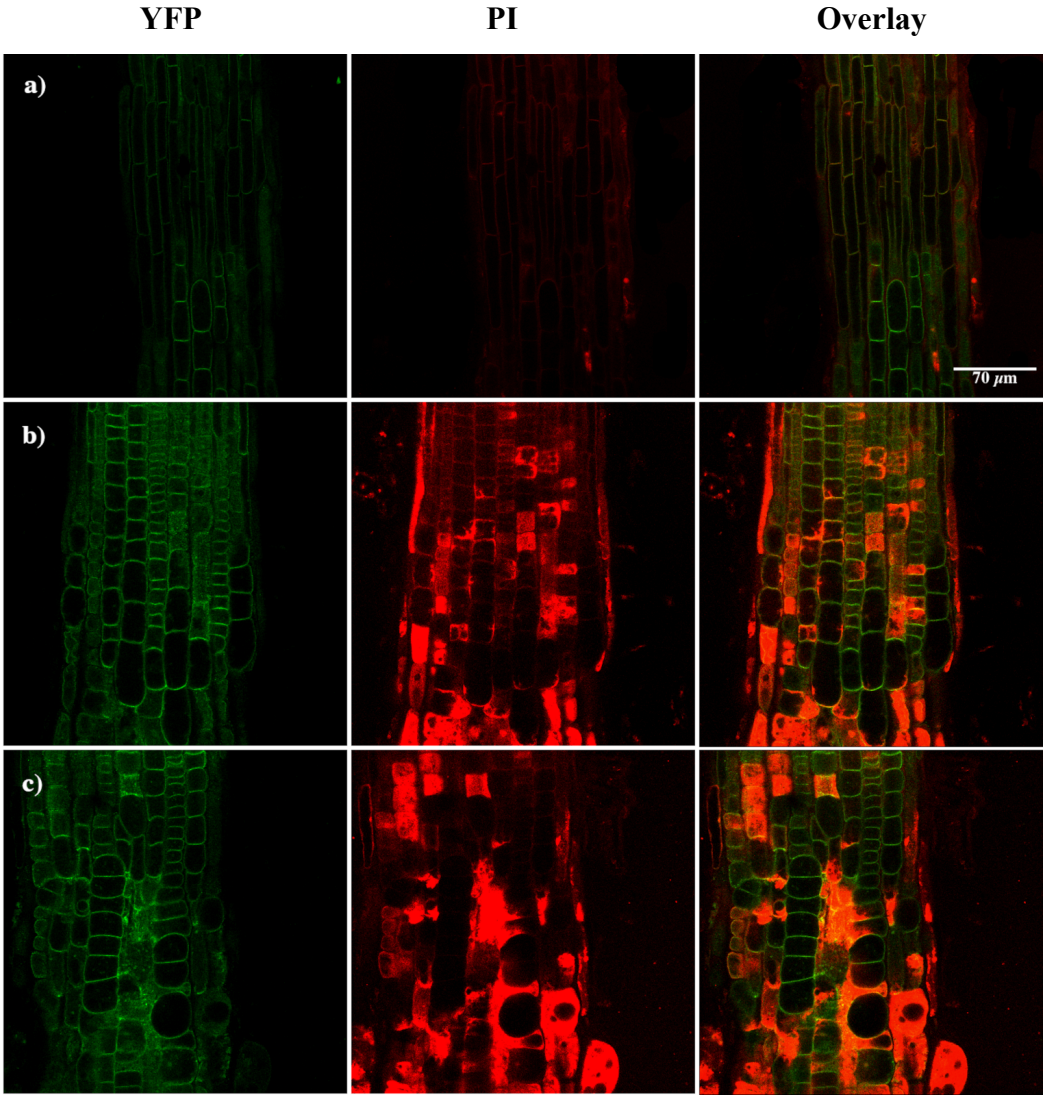

Figure 3.8: ISX + sorbitol-treated Wave 131Y seedlings stained with PI. Seedlings have been treated with ISX + sorbitol for **a)** 3 hours, **b)** 5 hours and **c)** 7 hours.

3.2.5 Comparing the effects of mock, ISX- and ISX + sorbitol-treatments

To facilitate comparison of the treatment effects the data available for 5 and 7 hours was compiled in the figures below. The mock-treated cells show anisotropic growth after 5 hours, where they grow mostly in the longitudinal direction compared to the radial direction, and the PM and cell wall are mostly straight, not curvy (figure 3.9 a). ISX-treatment seems to induce changes in cell shape, making the cells swell until some of them look almost circular, and with PI staining indicating some cell death (figure 3.9b). ISX + sorbitol-treatment looks to have milder effects on seedling cell shape because the cells look less swollen. This could be caused by the hyper-osmotic effect of sorbitol dampening the effect of ISX. On the other hand, it seems there is more intracellular staining of PI, indicating cell death (figure 3.10 c), meaning the overall condition of the cells may be worse than under just the ISX-treatment.

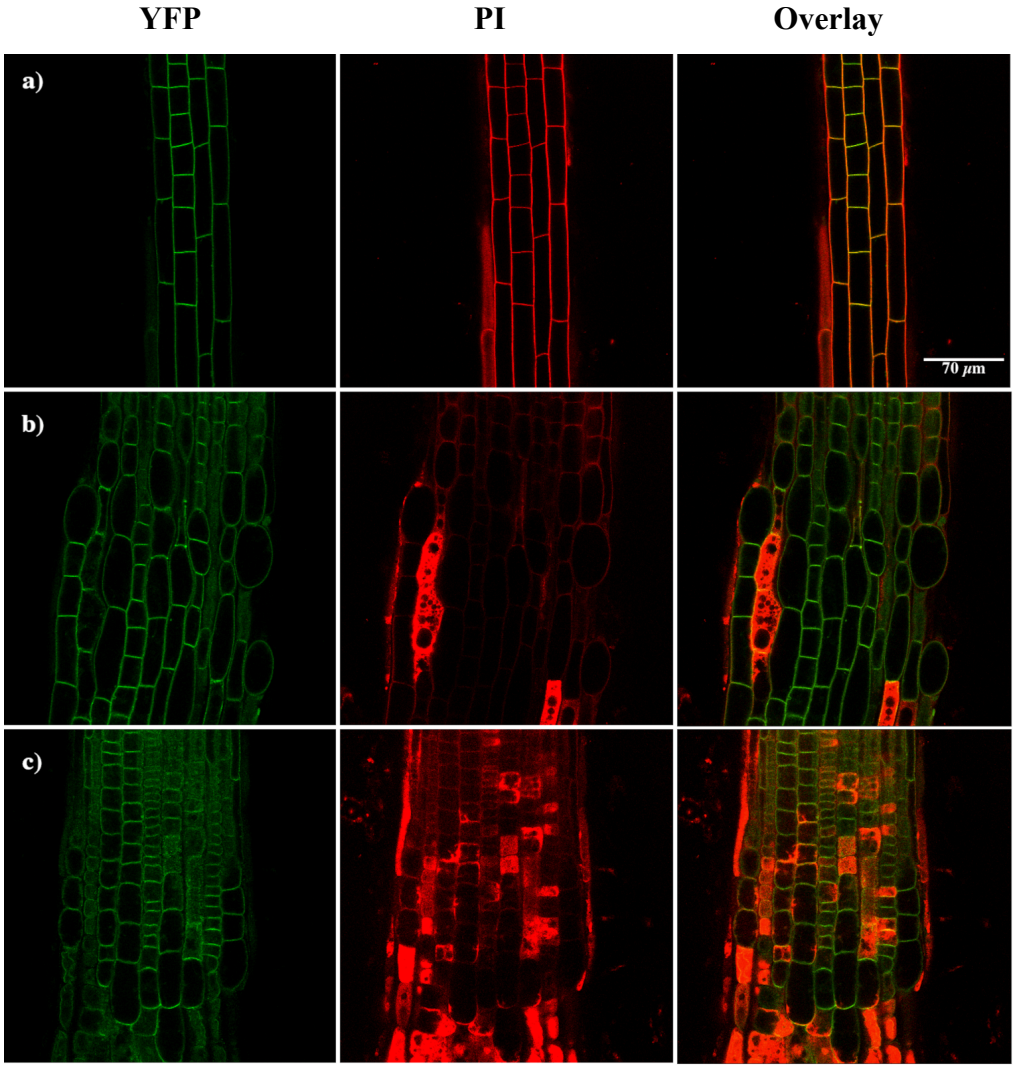

Figure 3.9: Comparison of Wave 131Y seedlings stained with PI and treated with different solutions for 5 hours **a)** A mock-treated seedling. **b)** an ISX-treated seedling. **c)** an ISX + sorbitol-treated seedling.

At the 7 hours timepoint, ISX-treated root cells are swollen compared to mock-treated ones (figure 3.10 a and b). There is also intracellular PI staining. ISX + sorbitol-treated cells seem less swollen than ISX-treated ones but more than mock-treated controls (figure 3.10 c). The intracellular PI staining seems more pronounced in the ISX + sorbitol-treated seedlings than in ISX alone, suggesting the physiological states of the cells are not necessarily better even though there is less swelling. In several of the cells exhibiting intracellular PI staining the YFP signal also appears to be filling the whole cell, not just the outline. This applies to both the ISX and ISX + sorbitol-treated cells. The reason for this may be that the focus of the picture is on the upper side of the cell from the microscope view.

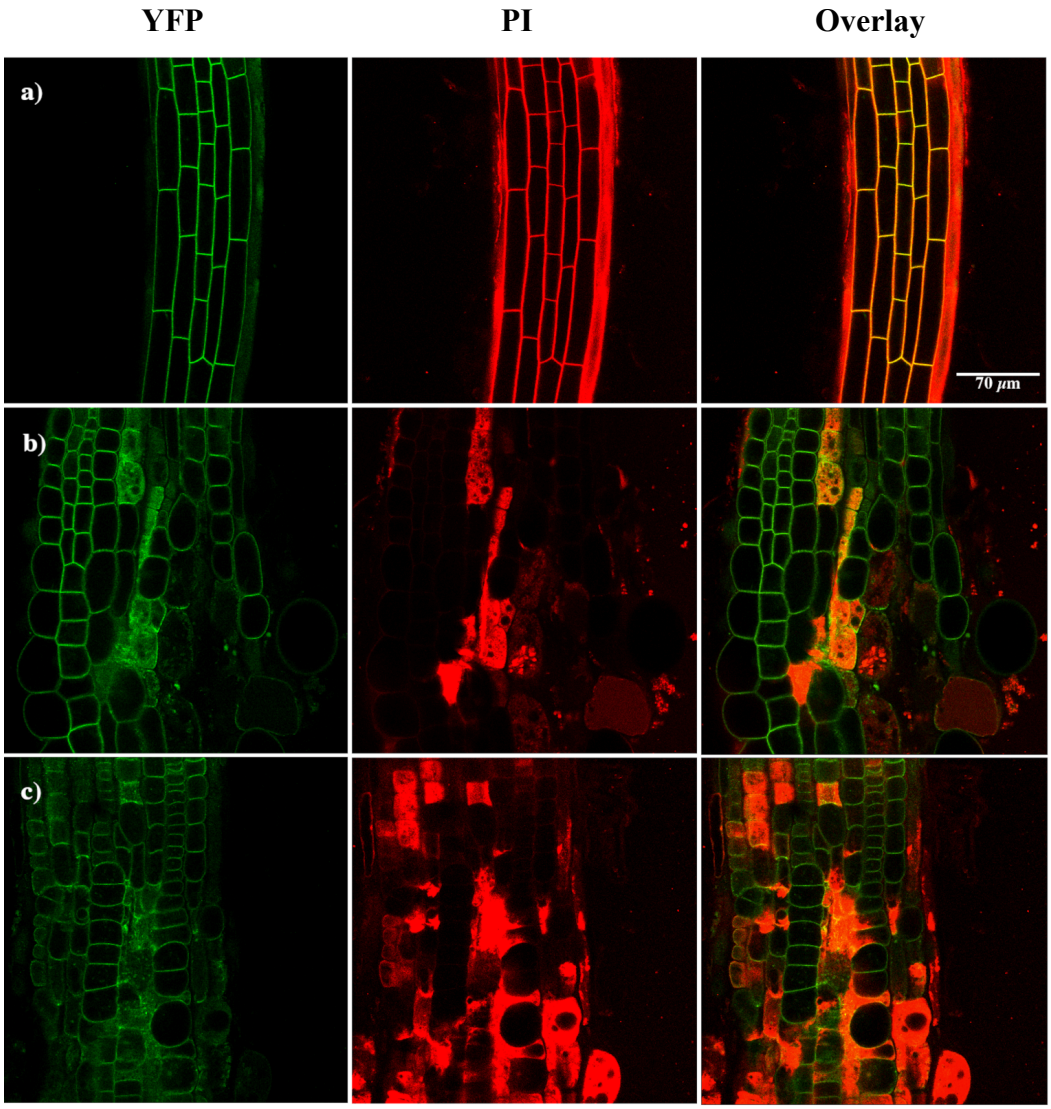

Figure 3.10: Comparison of Wave 131Y seedlings stained with PI and treated with different solutions for 7 hours. **a**) mock-treated root; **b)** ISX-treated root; **c)** ISX + sorbitol-treated root.

3.3 Fluorescent lifetime imaging microscopy of Flipper-TR stained seedlings

FLIM was conducted using 6 days old seedlings stained with Flipper-TR, then treated with either mock-, sorbitol- , ISX- or ISX + sorbitol-solutions, to look at differences in membrane tension. Lifetime was measured at 5, 60, 90, 120, 180, 240, 300, 360, 420 and 480 min for mock- and ISX-treatments. For sorbitol-treated seedlings lifetimes were measured at timepoints 5, 60, 90, 120 and 180 min. For ISX + sorbitol-treated seedlings lifetimes were measured at 180, 300 and 420 min (figure 3.11; Appendix 2, table A.2).

3.3.1 Fluorescent lifetime of Flipper-TR stained and mock treated seedlings

The fluorescent lifetimes of Flipper-TR-stained seedlings are between 3.25 and 4.25 ns for all the mock treated seedlings. The 5 min and 60 min timepoint have a distribution over 0.75 ns for measured lifetimes with the mean a bit longer than 3.7 ns. The 90, 120 and 180 min timepoints has smaller distribution, where lifetimes are distributed over around 0.5 ns (90 and 120 min), and around 0.6 ns (180min), all with the means around 3.7 ns (Appendix 2: figure A.1 for line chart). At 240 min the distribution is small, but it has only 6 biological replicates. The average lifetimes of the seedlings measured at 300 min and later seem to be shorter than the lifetime of the seedlings measured before 300 min. This suggests that the membrane tension of the epidermal cells may lessen over time. However, only the lifetime differences measured at 60 min and at 480 min are statistically significant different ($p = 0.0257$, Appendix 3: table A.3).

3.3.2 Fluorescent lifetime of Flipper-TR stained and ISX treated seedlings

Fluorescent lifetimes of Flipper-TR-stained ISX-treated seedlings are between 3.25 and 4.0 ns. At 5, 60 90 and 120 min the distribution of lifetimes covers around 0.5 ns, with means around 3.7 ns except at 60 min where the mean lifetime is closer to 3.8 ns. Lifetime distribution at timepoint 180 covers more than 0.5 ns, but the mean lifetime is under 3.6 ns. The distributions of lifetimes are smaller for the next timepoints, being around 0.25 ns for lifetimes at 240, 300, 360 and 420 min. For 480 min it is closer to 0.4 ns. The mean lifetimes continue to shorten also, with 480 min having the shortest mean lifetime (slightly over 3.4 ns). Lifetime measurements at 420 and 480 min are significantly lower compared to measurements made at 5, 60, 90 and 120 min. and lifetimes measured at timepoint 360 min are significantly lower than lifetimes measured at timepoint 60 min (Appendix 3: table A.4 for p-values). To

summarize these results, they suggest that the membrane tension is getting lower over time in ISX-treated seedlings in a noticeable manner.

3.3.3 Fluorescent lifetime of Flipper-TR-stained and sorbitol treated seedlings

The measured fluorescent lifetimes of Flipper-TR-stained seedlings treated with sorbitol range between 4.27 and 3.47 ns. The distributions of the lifetimes for 5, 60 and 90 min are between 0.5- 0.75 ns, while they are under 0.5 ns for 120 and 180 minutes. The means of the lifetimes are all around 3.8 ns. No statistically significant differences are detectable between any of the timepoints measured (Appendix 3: table A.5 for p-values). The mean lifetime seems relatively stable around 3.8 ns, suggesting the membrane tension does not change notable for up to 180 min sorbitol-treatment. The caveat being that only measurements for up to 180 min of sorbitol-treatment have been performed.

3.3.4 Fluorescent lifetime of Flipper-TR stained and ISX + sorbitol treated seedlings

The measured fluorescent lifetimes of Flipper-TR-stained ISX + sorbitol-treated seedlings vary between 4.27 and 3.23 ns. 3.23ns is the lowest measured lifetime overall and over 0.25 ns lower than the second lowest lifetime for this treatment and timepoint (300 min). The distributions of lifetimes are between 0.25-0.5 ns. The lifetime means range from around 3.9 ns for 180 min treatment to around 3.8 ns for 300 and 420 min treatment. There are no statistically significant differences detectable between any of the timepoints (Appendix 3: table A.6 for p-values), suggesting that the membrane tension is not changing significantly in the 3-7 hour period of treatment.

3.3.5 Comparison of fluorescent lifetimes between treatments

A statistical analysis was performed to determine if mock, ISX-, sorbitol and ISX + sorbitol-treatments have differential effects on plasma membrane tension in seedling root cells. The fluorescent lifetimes of seedlings treated with ISX + sorbitol differ significantly from mock- or ISX-treated ones at corresponding timepoints (Appendix 3: table A.7 for p-values) This seems to indicate that the membrane tension is significantly higher in ISX+ sorbitol-treated seedlings than those mock- or ISX- treated. Fluorescent lifetimes at timepoints 240, 360 and 420 min in mock-treated roots are statistically significant different from those in ISX-treated

ones at corresponding timepoints. This suggests the mock-treated seedlings have a significantly higher membrane tension than ISX treated seedlings. ISX- and sorbitol-treated seedlings have statistically significant differences in lifetime at timepoints 90 min and 180 min, but not for 120 min.

To summarize the mock-treated seedlings exhibit shorter lifetimes at later timepoint, implying a decrease in membrane tension over time. However, this trend is not pronounced based on the statistical analysis. In contrast the trend towards shorter lifetimes is pronounced in ISX-treated seedlings. It seems also like ISX + sorbitol-treated seedlings exhibit higher fluorescence lifetimes, thus higher membrane tension, than mock- or ISX-treated ones. It is important to note that in short-term sorbitol and longer-term ISX-sorbitol treated seedlings lifetimes are similarly elevated suggesting that in both elevated membrane tension exist. Importantly that also indicates that the presence of sorbitol is sufficient to suppress the reduction in lifetimes observed in ISX-treated seedlings.

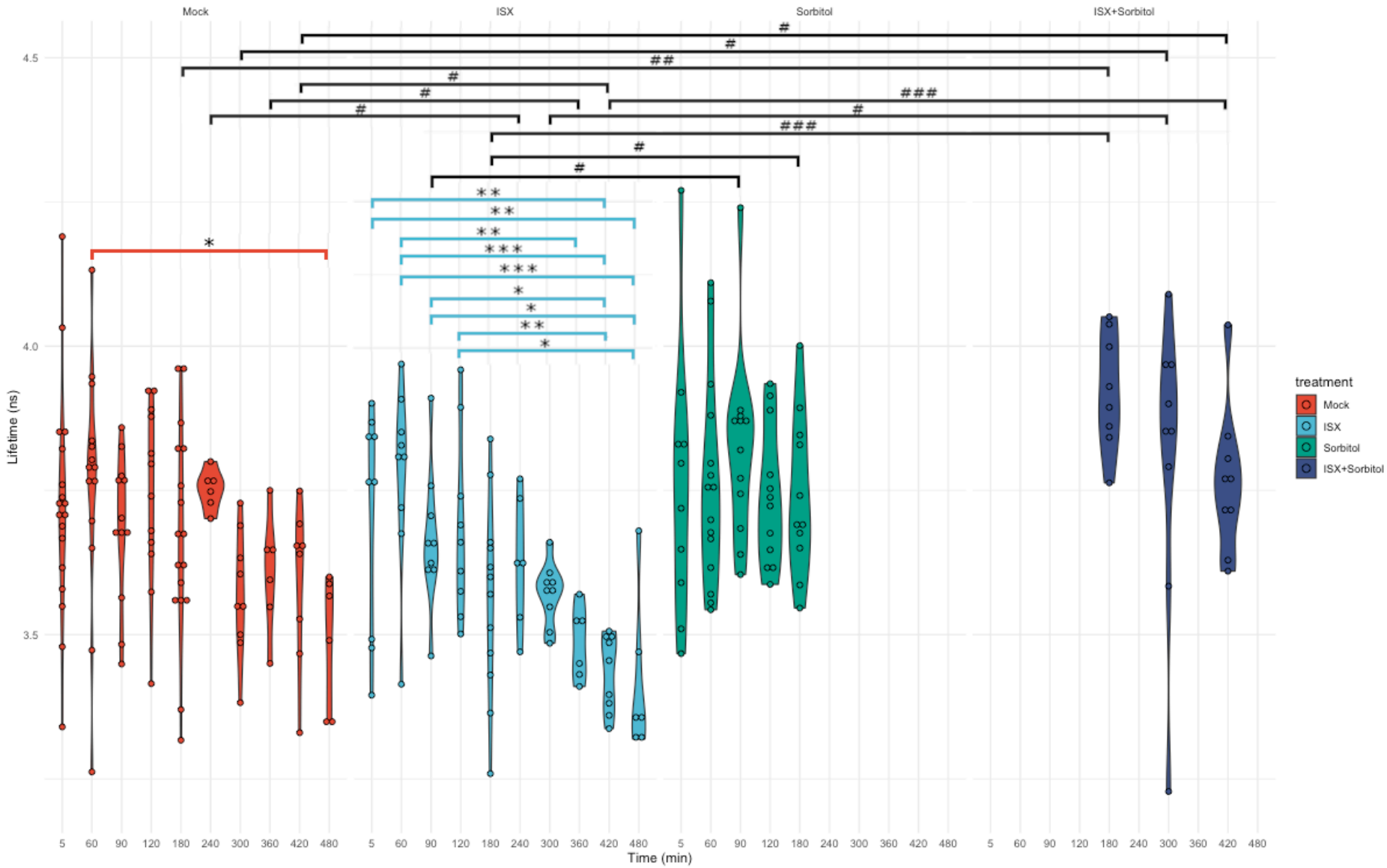

Figure 3.11: Violin plot of measured lifetimes. (*Continued on next page*)

Violin plots of the lifetime (ns) of Col-0 seedlings stained with Flipper-TR. mock treated (red). ISX (light blue). sorbitol (green) or ISX + sorbitol (dark blue). Lifetimes were measured at timepoints listed on X-axis. For mock-treated samples data derive from seven independent experiments with n = 18. n = 14. n = 12. n = 12. n = 17. n = 6. n = 9. n = 6. n = 8 and n = 6 biological replicates for timepoints 5 min, 60 min, 90 min, 120 min, 180 min, 240 min, 300 min, 360 min, 420 min and 480 min. For ISX: data derive from five independent experiments with n = 9, n = 9, n = 9, n = 9, n = 12, n = 6, n = 9, n = 6, n = 9 and n = 6 biological replicates for timepoints mentioned above. For sorbitol-treated samples data derive from four independent experiments. with n = 10, n = 15, n = 12, n = 12 and n = 11 biological replicates for timepoints 5 min. 60 min. 90 min. 120 min and 180 min respectively. For the ISX + sorbitol-treated samples data were generated in one experiment. with n = 8, n = 9 and n = 9 biological replicates for timepoints 180 min, 300 min and 420 min. Asterisks (*) or hash (#) (*/#: $p < 0.05$. **/##: $p < 0.01$. ***/###: $p < 0.001$) indicate a statistically significant difference between timepoints for a treatment (* and red (mock) and blue (ISX) brackets) or between treatments at a timepoint (# and black brackets). Statistical significance was found doing a one-way ANOVA followed by using Tukey s honestly significant difference (HSD) post hoc test ($\alpha = 0.05$). Non-significant differences are not shown.

4. Discussion

The plant cell needs to monitor and maintain the functional integrity of the surrounding cell wall in order to ensure survival (Bacete & Hamann, 2020). Based on previous work it has been hypothesized that the plasma membrane and/or interactions of membrane – cell wall continuum are involved in monitoring of the wall (Vaahtera et al., 2019). The monitoring could for example involve detection of changes in membrane tension or displacement of the PM relative to the cell wall. For instance, several mechanosensitive or stretch-activated ion channels may detect this change in tension. Representative examples for channels are MCA1 or OSCA1, which is another ion channel that induces cytosolic Ca^{2+} increase in response to hyper-osmotic stress (Bacete & Hamann, 2020; Haswell & Verslues, 2015). Flipper-TR has been used to study changes in membrane tension in mammalian and yeast cells (Colom et al., 2018; Roffay et al., 2021). It was therefore considered to be an attractive tool to study the membrane tension in plants. Here it was investigated if Flipper-TR is suitable to study the membrane tension changes in plants. This involved establishing treatment conditions and inducing changes in plasma membrane tension through either hyper-osmotic stress or ISX-treatments. These studies were correlated with an analysis of how the same treatments affect cell integrity and morphology over a similar period of time.

4.1 Validation of Flipper-TR, characterization of spectral properties and testing of experimental conditions

To confirm that Flipper-TR works as previously described a spectrum of the maximum excitation and emission wavelengths was made. The excitation emission spectra confirm Flipper-TR works in HaCaT cells as described by Colom et al. (2018), with and excitation maximum around 488 nm and emission maximum around 600 nm. This was hypothesized to apply for Flipper-TR in plants as well considering that the fluorophore has been used in yeast, e.g., by Riggi et al. (2018) which, for instance, has a cell wall exhibiting similar rigidity like a plant cell wall.

PBS and ½ MS were both tested as solvent for the Flipper-TR staining solution, since PBS was used when doing proof-of-concept testing in plant cells and ½ MS is the culture media commonly used for growth of seedlings. One hour of treatment showed PI staining inside most of the PBS-treated cells, indicating cell death, while the ½ MS-treatment showed no signal inside the cells. While PBS is infrequently used as a solvent when using whole plant samples,

it has been used before as control solution (Niehl et al., 2016) when studying pattern-triggered immunity in *Arabidopsis*. The extent of cell damage observed in PBS treated seedlings was therefore unexpected. The pH of PBS is around 7.2, which is higher than the ½ MS pH of 5.7. However, the pH of the apoplast in *Arabidopsis* root cells can range from 5-7. Furthermore, roots have to be able to adapt to different pH as it traditional growth media, soil, can vary greatly in pH from one area to another (Martinière et al., 2018). It is therefore not likely the change in pH should cause the amount of damage observed.
In animal cells, PBS have been found to increase shear stress leading to a decrease in viability (Chen et al., 2017; Sargent et al., 2021). While it has not been studied yet, it is possible that chemicals which induce shear stress might impact cell-to-cell adhesion. Shear stress has been used to study plant cell – substrate adhesion (Atakhani et al., 2022), so it is a possibility that increased shear stress would impact cell-cell adhesion as well. This would need to be studied further before anything could be concluded, especially considering the mechanics of cell-to-cell adhesion differs in plant and animal cells (Atakhani et al., 2022).

It is also apparent that a 2 % (*v/v*) concentration of DMSO in the staining solution is not optimal, based on the damage seen in certain the root cells. DMSO has been found to induce thinning and expansion of the plasma membrane while decreasing rigidity and tension of the PM, promoting permeability (Gurtovenko & Anwar, 2007). With higher concentrations of DMSO (10-20 mol %) there is also formation of temporary water pores (Gurtovenko & Anwar, 2007). Therefore, it cannot be ruled out that these effects were affecting seedlings treated with 2 % DMSO diluted in ½ MS. Optimally, there would be no or a much smaller concentration of DMSO used during plant tissue staining. However, the current Flipper-TR probe and conditions required for staining seedlings necessitated the high DMSO concentration in the staining solution. In mammalian cells, a much lower concentration of Flipper-TR is necessary for staining, maybe because often only a single cell layer is being stained, and the extracellular matrix is much thinner than a cell wall. Hopefully in the future, improvements will be made so the Flipper-TR probe can either be diluted in other solvents or smaller concentrations are required to stain seedlings.

Flipper-TR has been used before in organisms, which can grow in a single cell layer, unlike a plant root, which has several cell layers. It was therefore not an entirely unexpected outcome that the fluorophore did not penetrate to inner tissues below the first cell layer, and the FLIM measurements had to be taken of the epidermal cell layer. A comparable situation exists for PI

staining, where the Casparian strip blocks the dye from entering the central cylinder (Naseer et al., 2012). The reason for Flipper-TR not diffusing into the inner cell layers remains to be determined

4.2 Comparison of treatment effects using Wave 131Y expressing seedlings

In parallel to the studies using Flipper-TR the treatment effects on epidermal cells were studied. Based on previously published results, it was expected to see cell swelling in seedlings treated with ISX for about 4-5 hours, maybe see changes in the cells treated with sorbitol, and see less pronounced swelling if seedlings were co-treated with sorbitol and ISX. Wave 131Y seedlings were used in combination with PI to visualize the effect of the treatments on the cell wall, the PM and cell viability. PI binds to demethoxylated pectins of the cell wall while the membrane is intact (Rounds et al., 2011). However, if the cell membrane is damaged the PI can leak into the cell through the now permeable membrane and stain nucleic acids (Guo et al., 2014). Because of this, PI can be used as a indicator for cell vitality (Rounds et al., 2011).

For the sorbitol-treatment, seedlings were only imaged for timepoints 1, 2 and 3 hours. The reasons being that earlier studies showed that ABA production is induced after 3 hours of sorbitol-treatment (Bacete et al., 2022). Additionally, *THIC* and *THI1* (genes responsible for the biosynthesis of the pyrimidine and thiazole moieties of thiamine (vitamin B_1)) are upregulated after 2 hours of 200 mM sorbitol-treatment (Rapala-Kozik et al., 2012).
Comparison of the PI signal in seedlings treated with sorbitol for 1 hour vs 3 hours imply that the treatment damages the PM of the cells, with more damaged cells visible after 3 hours. Ca^{2+} influx from the apoplast into the cytosol happens after biotic and abiotic stress, e.g. mechanical stress, and before programmed cell death (Ren et al., 2021). It has also been shown that a decrease in Ca^{2+} enhances the PI signal, since Ca^{2+} and PI are thought to interact with the same binding sites and a high Ca^{2+} concentration hinder PI from intercalating with pectins (Rounds et al., 2011). It is therefore a possibility that if the stress, such as mechanical damage, lead to a cytosolic influx of enough Ca^{2+} causing the concentration to noticeably fall in the apoplast, PI will have more binding sites which again will lead to a stronger signal. This would explain why some of the cell borders have more intense PI signal and raises the question if this signal really indicates cell death. The PI signal in the sorbitol-treated seedlings also looks similar to what has been described as cell death in other seedlings (Hong et al., 2017). While 300 mM sorbitol

significantly affects plant growth it is not enough to kill it outright, as seedlings can survive for at least 30 days (Zhang et al., 2013).

The effects of the ISX-treatments were visualized every hour between 4 and 7 hours. ISX-treatment clearly causes swollen epidermal cells after 5 hours. There might be already some swelling after 4 hours, but to determine if there is a difference between the mock- and the ISX-treatment, a quantitative study of the cell wall shape is required where longitudinal and radial ratio are compared for both treatments using an adequate number of cells. This have been done in cells in the transition zone before, but not in epidermis cells (Gigli-Bisceglia et al., 2018). It would therefore not be surprising to detect a difference after 4 hours, as morphological effects of ISX have been detected before 4 hours of treatment (Gigli-Bisceglia et al., 2018; Hamann et al., 2009). There appears to be more and more cell damage, indicated by intracellular PI signal, the longer the seedlings are exposed, with cell death first being seen after 5 hours of exposure. In some instances, the cell membrane looks more intact than in other. This is exemplified by a cell filled with PI stain visible in the bottom right picture after 7 hours of treatment (Fig. 3.7 d), which appears not to have any intracellular YFP staining, while other cells apparently have both PI and YFP signal. More detailed studies are necessary to understand what is happening.

For the ISX + sorbitol-treatments, seedlings were imaged at 3, 5 and 7 hours so that the effect of the double treatment could be compared to both the individual sorbitol and ISX-treatments. 3 hour treatments for sorbitol and ISX + sorbitol have similar effect. Both exhibit some cell PI signal indicating cell damage, which is likely caused by the sorbitol in the co-treatment as ISX probably has limited effects after 3 hours.
After both 5 and 7 hours of treatments seedling roots exhibit clearly more PI and YFP signal, likely indicating cell damage/death. The PI stain is similar to what is described as cell death after 14 hour 100 mM NaCl-treatment in a root tip by Oh et al. (2010), which may indicate this damage is caused by osmotic stress. The reason we did not see this extent of damage in the sorbitol-treatment may be because the seedlings were not exposed for a long enough time. On the other hand, there seems to be less swelling than for ISX alone, likely because the hyper-osmotic sorbitol-treatment is dampening the effect turgor has on a weakened cell wall, which has been reported before (Bacete et al., 2022; Engelsdorf et al., 2018). This would suggest that physical properties of the PM or the PM – cell wall continuum have to be disturbed, enabling the cell to perceive the effect of ISX on CWI.

The mock-treatment have no effects on the root cells, with no visible swelling or intracellular YFP or PI signal detectable at any of the time points examined. This was expected as ½ MS is a commonly used growth media for *Arabidopsis* and the same media used when growing the seedlings for this experiment. The only difference being 0.1% DMSO, which was included in both the mock and sorbitol-treatments so the results could be comparable to the treatments with ISX. This low concentration of DMSO does not seem to have an effect on the root, unlike treatments with 2% DMSO used for Flipper-TR. DMSO has been reported to decrease membrane thickness in concentrations as low as 2.5 mol % (Gurtovenko & Anwar, 2007). However, lipid bilayers comprising zwitterionic dipalmitoylphosphatidylcholine (DPPC) lipids in aqueous solution were used to get these results, not a cell membrane in a living cell, so the effects in a living cell might be different (Gurtovenko & Anwar, 2007).

JA is induced in response to plant defense, e.g., in response to wound damage and to the related response to mechanical damage (Zou et al., 2016). What perceives the stimulus arising from mechanical damage or how the JA biosynthesis is activated is not well understood (Zou et al., 2016). However, there are indications that the JA pathway is triggered by mechanical changes resulting from wall weakening (Mielke et al., 2021). Also, the mechanosensitive ion channel MscS-like 10 (MSL10), localized in the PM, has been implicated in wound-triggered early signal transduction pathways, and there may be positive feedback regulation of JA biosynthesis (Zou et al., 2016). ISX-treatment induces JA production, but with sorbitol co-treatment JA accumulation is suppressed (Engelsdorf et al., 2018). The PMs of seedlings treated with ISX probably expand when the cell wall weakens, and the turgor pressure forces the cell to swell. If mechanical displacement / cell wall expansion is (partly) responsible for the induction of JA, it would explain why sorbitol repress JA accumulation in co-treatment with ISX. The reason being that the hyper-osmotic stress reduces PM and cell wall expansion which happens in response to ISX-treatment. The lack of JA accumulation in ISX + sorbitol-treated cells may then also explain why there is more cell death in the co-treated cells than upon ISX-treatment alone, since adaptive responses normally triggered by JA to mitigate the effects of the stress are not activated (Koo & Howe, 2009).

4.3 Fluorescent lifetime imaging microscopy of Flipper-TR stained seedlings

Even though DMSO affects PM organization, it is still possible to compare the different treatments with each other because all the seedlings were exposed to DMSO/stained in the same manner.

Measurements in mock-treated seedlings indicate a reduction in lifetimes over time, suggesting a reduction in membrane tension. After 240, 360 and 420 minutes of ISX-treatment the lifetimes measured in seedlings are significantly shorter than for the mock-treatment, indicating lower membrane tension. These results suggest that ISX seems to have a specific effect on the membrane tension by itself.

The lifetimes measured in seedlings treated with ISX + sorbitol were significantly higher than for both the ISX- and the mock-treatment at timepoints 180, 300 and 420 min. Interestingly, they were similar to the lifetimes observed after 180 min of sorbitol-treatment. Lifetime measurements from the short-term sorbitol-treatments are also significantly higher than for mock or ISX. All this shows that the ISX + sorbitol-treatment effects are closer to the sorbitol effects than to ISX. It also indicates that sorbitol can suppress the ISX-induced decreased PM tension in seedlings (section 4.2). These results hint at a molecular structure, located at the PM or PM – cell wall continuum, being important in the perception of CWI impairment.

It would be interesting to have additional measurements from timepoints after 180 min treatment for sorbitol and before 180 min for the sorbitol- and ISX + sorbitol-treatment, to be able to compare the different treatments more thoroughly.

An increased lifetime indicates an increase in membrane tension, and a decrease in lifetime indicates a decrease in membrane tension. Hyper-osmotic treatments (induced by sorbitol) are expected to cause less tension in the PM while an ISX-treatment (possibly comparable to hypo-osmotic treatment) is expected to cause more tension in the PM. This is based on results found earlier when using mammalian and yeast cells (Colom et al., 2018; Roffay et al., 2021). Here however, the ISX-treatment decreased the Flipper-TR lifetime. Sorbitol-treatment is not significantly higher at early time points compared to mock. However, ISX + sorbitol has a significantly higher lifetime than both mock and ISX. This is the opposite of what has been observed in mammalian and yeast cells. This is on the other hand what was found to happen in single lipid phase membranes (Colom et al., 2018).

Technically the lipid packing, not the membrane tension itself, is detected using Flipper-RT. The combination of the treatments with the experimental conditions (2% DMSO), may be the cause for this result. The results could be explained in the following manner. If the DMSO is already decreasing the rigidity and tension of the PM (decreasing trend for lifetimes with time in mock samples), the sorbitol-treatment may cause the membrane to contract slightly, which would make the lipid bilayer compress and thus making more of the membrane go from lipid disorder to lipid order (Colom et al., 2018). The ISX-treatment could then force the membrane to go from consisting of more lipid disordered phase than in mock, to even more disordered when the cell wall weakens, and the turgor pressure forces the membrane to expand.
The results from the mock-treatment might suggest the transfer from a high DMSO concentration to the mock-treatment is not enough to reverse the effects, but rather the PM rigidity and tension keep decreasing, causing the lifetime to decrease too. However, further studies are needed to figure out exactly what is happening.

4.4 Conclusion and future work

Here, morphological changes in seedlings exposed to hyperosmotic stress and ISX-treatments were investigated using a reporter construct. In addition, the conditions for using Flipper-TR in plants to characterize changes in plasma membrane tension were established. ½ MS was found to be the best solvent for the staining solution and osmotic treatments, while the DMSO concentration necessary for staining was found to be detrimental to the cells. Lifetimes of the stain were measured in epidermal root cells using FLIM. It was found that the ISX + sorbitol-treatment had significantly different effects compared to ISX- and mock-treatment, with ISX-treatment likely causing a decrease in lifetime whereas sorbitol likely contributes to a higher lifetime. Both the morphological changes from ISX + sorbitol treated Wave 131Y seedlings stained with PI and the lifetime measurements, imply that sorbitol dampens the effect of ISX on seedlings. These results indicate that osmo-sensitive mechanisms are important in perception of CWI impairment and imply that mechano-perception is relevant as well.
Furthermore, the high DMSO concentration in the Flipper-TR staining solution may be the cause why the lifetimes measured for the different treatments behaved opposite to what has been observed in mammalian and yeast cells. However, this remains to be determined since there should be other molecular mechanisms responsible for this change in the lipid packing of the plasma membrane.

In the future, it would be interesting to look at the JA induction in connection with PM – cell wall displacement, and the role of mechanosensing ion channels. To be able to better compare the effect the different treatments have on the lifetime of the epidermal cells, measuring the lifetime of seedlings exposed to sorbitol-treatment for longer than 3 hours, and ISX + sorbitol-treatment for shorter than 3 hours would be instructive.
Importantly, the usability of Flipper-TR must be improved. Here the focus should be on using a different solvent or lower concentrations of the currently used solvent.

References

Ackermann, F., & Stanislas, T. (2020). The plasma membrane—an integrating compartment for mechano-signaling. *Plants, 9*(4), 505.

Anderson, C. T., & Kieber, J. J. (2020). Dynamic construction, perception, and remodeling of plant cell walls. *Annual Review of Plant Biology, 71*, 39-69.

Assies, L., García-Calvo, J., Piazzolla, F., Sanchez, S., Kato, T., Reymond, L., . . . Straková, K. (2021). Flipper Probes for the Community. *CHIMIA International Journal for Chemistry, 75*(12), 1004-1011.

Atakhani, A., Bogdziewiez, L., & Verger, S. (2022). Characterising the mechanics of cell–cell adhesion in plants. *Quantitative Plant Biology, 3*.

Aydinalp, C., & Cresser, M. S. (2008). The effects of global climate change on agriculture. *American-Eurasian Journal of Agricultural & Environmental Sciences, 3*(5), 672-676.

Bacete, L., & Hamann, T. (2020). The Role of Mechanoperception in Plant Cell Wall Integrity Maintenance. *Plants, 9*(5), 574.

Bacete, L., Schulz, J., Engelsdorf, T., Bartosova, Z., Vaahtera, L., Yan, G., . . . Gigli-Bisceglia, N. (2022). THESEUS1 modulates cell wall stiffness and abscisic acid production in Arabidopsis thaliana. *Proceedings of the National Academy of Sciences, 119*(1).

Chaudhary, A., Chen, X., Gao, J., Leśniewska, B., Hammerl, R., Dawid, C., & Schneitz, K. (2020). The Arabidopsis receptor kinase STRUBBELIG regulates the response to cellulose deficiency. *PLoS genetics, 16*(1), e1008433.

Chen, A., Leith, M., Tu, R., Tahim, G., Sudra, A., & Bhargava, S. (2017). Effects of diluents on cell culture viability measured by automated cell counter. *PloS one, 12*(3), e0173375.

Colom, A., Derivery, E., Soleimanpour, S., Tomba, C., Dal Molin, M., Sakai, N., . . . Roux, A. (2018). A fluorescent membrane tension probe. *Nature chemistry, 10*(11), 1118-1125.

Daher, F. B., & Braybrook, S. A. (2015). How to let go: pectin and plant cell adhesion. *Frontiers in plant science, 6*, 523.

Datta, R., Gillette, A., Stefely, M., & Skala, M. C. (2021). Recent innovations in fluorescence lifetime imaging microscopy for biology and medicine. *Journal of biomedical optics, 26*(7), 070603.

Datta, R., Heaster, T. M., Sharick, J. T., Gillette, A. A., & Skala, M. C. (2020). Fluorescence lifetime imaging microscopy: fundamentals and advances in instrumentation, analysis, and applications. *Journal of biomedical optics, 25*(7), 071203.

de Almeida, R. F., Loura, L. M., & Prieto, M. (2009). Membrane lipid domains and rafts: current applications of fluorescence lifetime spectroscopy and imaging. *Chemistry and physics of lipids, 157*(2), 61-77.

Denness, L., McKenna, J. F., Segonzac, C., Wormit, A., Madhou, P., Bennett, M., . . . Hamann, T. (2011). Cell Wall Damage-Induced Lignin Biosynthesis Is Regulated by a Reactive Oxygen Species- and Jasmonic Acid-Dependent Process in Arabidopsis *Plant physiology, 156*(3), 1364-1374. doi:10.1104/pp.111.175737

Desprez, T., Juraniec, M., Crowell, E. F., Jouy, H., Pochylova, Z., Parcy, F., . . . Vernhettes, S. (2007). Organization of cellulose synthase complexes involved in primary cell wall synthesis in Arabidopsis thaliana. *Proceedings of the National Academy of Sciences, 104*(39), 15572-15577.

Engelsdorf, T., Gigli-Bisceglia, N., Veerabagu, M., McKenna, J. F., Vaahtera, L., Augstein, F., . . . Hamann, T. (2018). The plant cell wall integrity maintenance and immune signaling systems cooperate to control stress responses in Arabidopsis thaliana. *Science signaling, 11*(536).

Furt, F., Simon-Plas, F., & Mongrand, S. (2011). Lipids of the plant plasma membrane. In *The plant plasma membrane* (pp. 3-30): Springer.

Ge, Z., Dresselhaus, T., & Qu, L.-J. (2019). How CrRLK1L receptor complexes perceive RALF signals. *Trends in plant science, 24*(11), 978-981.

Gerland, P., Raftery, A. E., Ševčíková, H., Li, N., Gu, D., Spoorenberg, T., . . . Lalic, N. (2014). World population stabilization unlikely this century. *Science, 346*(6206), 234-237.

Gigli-Bisceglia, N., Engelsdorf, T., & Hamann, T. (2020). Plant cell wall integrity maintenance in model plants and crop species-relevant cell wall components and underlying guiding principles. *Cellular and Molecular Life Sciences, 77*(11), 2049-2077.

Gigli-Bisceglia, N., Engelsdorf, T., Strnad, M., Vaahtera, L., Khan, G. A., Yamoune, A., . . . Hejatko, J. (2018). Cell wall integrity modulates Arabidopsis thaliana cell cycle gene expression in a cytokinin-and nitrate reductase-dependent manner. *Development, 145*(19).

Gigli-Bisceglia, N., & Testerink, C. (2021). Fighting salt or enemies: shared perception and signaling strategies. *Current opinion in plant biology, 64*, 102120.

Gonneau, M., Desprez, T., Martin, M., Doblas, V. G., Bacete, L., Miart, F., . . . Landrein, B. (2018). Receptor kinase THESEUS1 is a rapid alkalinization factor 34 receptor in Arabidopsis. *Current Biology, 28*(15), 2452-2458. e2454.

Gronnier, J., Gerbeau-Pissot, P., Germain, V., Mongrand, S., & Simon-Plas, F. (2018). Divide and rule: plant plasma membrane organization. *Trends in plant science, 23*(10), 899-917.

Guo, X., Liu, J., & Xiao, B. (2014). Evaluation of the damage of cell wall and cell membrane for various extracellular polymeric substance extractions of activated sludge. *Journal of biotechnology, 188*, 130-135.

Gurtovenko, A. A., & Anwar, J. (2007). Modulating the structure and properties of cell membranes: the molecular mechanism of action of dimethyl sulfoxide. *The journal of physical chemistry B, 111*(35), 10453-10460.

Hamann, T., Bennett, M., Mansfield, J., & Somerville, C. (2009). Identification of cell-wall stress as a hexose-dependent and osmosensitive regulator of plant responses. *The Plant Journal, 57*(6), 1015-1026.

Hamilton, N. (2009). Quantification and its applications in fluorescent microscopy imaging. *Traffic, 10*(8), 951-961.

Haswell, E. S., & Verslues, P. E. (2015). The ongoing search for the molecular basis of plant osmosensing. *Journal of General Physiology, 145*(5), 389-394.

Hepler, P. K., & Gunning, B. E. (1998). Confocal fluorescence microscopy of plant cells. *Protoplasma, 201*(3), 121-157.

Higashi, Y., & Saito, K. (2019). Lipidomic studies of membrane glycerolipids in plant leaves under heat stress. *Progress in Lipid Research, 75*, 100990.

Hong, J. H., Savina, M., Du, J., Devendran, A., Ramakanth, K. K., Tian, X., . . . Xu, J. (2017). A sacrifice-for-survival mechanism protects root stem cell niche from chilling stress. *Cell, 170*(1), 102-113. e114.

Jonkman, J., & Brown, C. M. (2015). Any way you slice it—a comparison of confocal microscopy techniques. *Journal of biomolecular techniques: JBT, 26*(2), 54.

Koo, A. J., & Howe, G. A. (2009). The wound hormone jasmonate. *Phytochemistry, 70*(13-14), 1571-1580.

Lampugnani, E. R., Khan, G. A., Somssich, M., & Persson, S. (2018). Building a plant cell wall at a glance. *Journal of Cell Science, 131*(2), jcs207373.

Lee, K. J., Marcus, S. E., & Knox, J. P. (2011). Cell wall biology: perspectives from cell wall imaging. *Molecular plant, 4*(2), 212-219.

Lesk, C., Rowhani, P., & Ramankutty, N. (2016). Influence of extreme weather disasters on global crop production. *Nature, 529*(7584), 84-87.

Li, L., Xu, Y., Chen, Y., Zheng, J., Zhang, J., Li, R., . . . Chen, H. (2020). A family of push-pull bio-probes for tracking lipid droplets in living cells with the detection of heterogeneity and polarity. *Analytica Chimica Acta, 1096*, 166-173.

Li, Q., Wang, C., & Mou, Z. (2020). Perception of damaged self in plants. *Plant physiology, 182*(4), 1545-1565.

Liu, X., Lin, D., Becker, W., Niu, J., Yu, B., Liu, L., & Qu, J. (2019). Fast fluorescence lifetime imaging techniques: A review on challenge and development. *Journal of Innovative Optical Health Sciences, 12*(05), 1930003.

Lorrai, R., & Ferrari, S. (2021). Host cell wall damage during pathogen infection: Mechanisms of perception and role in plant-pathogen interactions. *Plants, 10*(2), 399.

M. Shotton, D. (1989). Confocal scanning optical microscopy and its applications for biological specimens. *Journal of Cell Science, 94*(2), 175-206.

Martinière, A., Gibrat, R., Sentenac, H., Dumont, X., Gaillard, I., & Paris, N. (2018). Uncovering pH at both sides of the root plasma membrane interface using noninvasive imaging. *Proceedings of the National Academy of Sciences, 115*(25), 6488-6493.

Mielke, S., Zimmer, M., Meena, M. K., Dreos, R., Stellmach, H., Hause, B., . . . Gasperini, D. (2021). Jasmonate biosynthesis arising from altered cell walls is prompted by turgor-driven mechanical compression. *Science Advances, 7*(7), eabf0356.

Minsky, M. (1988). Memoir on inventing the confocal scanning microscope. *Scanning, 10*(4), 128-138.

Mohnen, D. (2008). Pectin structure and biosynthesis. *Current opinion in plant biology, 11*(3), 266-277.

Nan Xiao (2018). ggsci: Scientific Journal and Sci-Fi Themed Color Palettes for 'ggplot2'. R package version 2.9. https://CRAN.R-project.org/package=ggsci

Naseer, S., Lee, Y., Lapierre, C., Franke, R., Nawrath, C., & Geldner, N. (2012). Casparian strip diffusion barrier in Arabidopsis is made of a lignin polymer without suberin. *Proceedings of the National Academy of Sciences, 109*(25), 10101-10106.

Niehl, A., Wyrsch, I., Boller, T., & Heinlein, M. (2016). Double-stranded RNA s induce a pattern-triggered immune signaling pathway in plants. *New Phytologist, 211*(3), 1008-1019.

Novaković, L., Guo, T., Bacic, A., Sampathkumar, A., & Johnson, K. L. (2018). Hitting the wall—Sensing and signaling pathways involved in plant cell wall remodeling in response to abiotic stress. *Plants, 7*(4), 89.

Nwaneshiudu, A., Kuschal, C., Sakamoto, F. H., Anderson, R. R., Schwarzenberger, K., & Young, R. C. (2012). Introduction to confocal microscopy. *Journal of Investigative Dermatology, 132*(12), 1-5.

Oh, D.-H., Lee, S. Y., Bressan, R. A., Yun, D.-J., & Bohnert, H. J. (2010). Intracellular consequences of SOS1 deficiency during salt stress. *Journal of experimental botany, 61*(4), 1205-1213.

Persson, S., Paredez, A., Carroll, A., Palsdottir, H., Doblin, M., Poindexter, P., . . . Somerville, C. R. (2007). Genetic evidence for three unique components in primary cell-wall cellulose synthase complexes in Arabidopsis. *Proceedings of the National Academy of Sciences, 104*(39), 15566-15571.

Prasad, P. N. (2003). *Introduction to biophotonics*: John Wiley & Sons.

Pritchard, J. (2007). Turgor pressure. In K. Roberts (Ed.), *Handbook of Plant Science, 2 Volume Set* (Vol. 1, pp. 148-151): John Wiley & Sons.

Rapala-Kozik, M., Wolak, N., Kujda, M., & Banas, A. K. (2012). The upregulation of thiamine (vitamin B1) biosynthesis in Arabidopsis thaliana seedlings under salt and osmotic stress conditions is mediated by abscisic acid at the early stages of this stress response. *BMC plant biology, 12*(1), 1-14.

R Core Team (2020). R: A language and environment for statistical computing. R Foundation for Statistical Computing, Vienna, Austria. URL https://www.R-project.org/.

Ren, H., Zhao, X., Li, W., Hussain, J., Qi, G., & Liu, S. (2021). Calcium signaling in plant programmed cell death. *Cells, 10*(5), 1089.

Riggi, M., Kusmider, B., & Loewith, R. (2020). The flipside of the TOR coin–TORC2 and plasma membrane homeostasis at a glance. *Journal of Cell Science, 133*(9), jcs242040.

Riggi, M., Niewola-Staszkowska, K., Chiaruttini, N., Colom, A., Kusmider, B., Mercier, V., . . . Roux, A. (2018). Decrease in plasma membrane tension triggers PtdIns (4, 5) P2 phase separation to inactivate TORC2. *Nature cell biology, 20*(9), 1043-1051.

Roffay, C., Molinard, G., Kim, K., Urbanska, M., Andrade, V., Barbarasa, V., . . . Matile, S. (2021). Passive coupling of membrane tension and cell volume during active response of cells to osmosis. *Proceedings of the National Academy of Sciences, 118*(47).

Roumeli, E., Ginsberg, L., McDonald, R., Spigolon, G., Hendrickx, R., Ohtani, M., . . . Daraio, C. (2020). Structure and biomechanics during xylem vessel transdifferentiation in Arabidopsis thaliana. *Plants, 9*(12), 1715.

Rounds, C. M., Lubeck, E., Hepler, P. K., & Winship, L. J. (2011). Propidium iodide competes with Ca2+ to label pectin in pollen tubes and Arabidopsis root hairs. *Plant physiology, 157*(1), 175-187.

RStudio Team (2019). RStudio: Integrated Development for R. RStudio, Inc., Boston, MA. URL http://www.rstudio.com/.

Sánchez-Rodríguez, C., Rubio-Somoza, I., Sibout, R., & Persson, S. (2010). Phytohormones and the cell wall in Arabidopsis during seedling growth. *Trends in plant science, 15*(5), 291-301.

Sargent, C. R., Perkins, I. L., Kanamarlapudi, V., Moriarty, C., & Ali, S. (2021). Hemodilution increases the susceptibility of red blood cells to mechanical shear stress during in vitro hemolysis testing. *ASAIO Journal, 67*(6), 632-641.

Savatin, D. V., Gramegna, G., Modesti, V., & Cervone, F. (2014). Wounding in the plant tissue: the defense of a dangerous passage. *Frontiers in plant science, 5*, 470.

Scheible, W.-R., Eshed, R., Richmond, T., Delmer, D., & Somerville, C. (2001). Modifications of cellulose synthase confer resistance to isoxaben and thiazolidinone herbicides in Arabidopsis Ixr1 mutants. *Proceedings of the National Academy of Sciences, 98*(18), 10079-10084.

Shin, Y., Chane, A., Jung, M., & Lee, Y. (2021). Recent Advances in Understanding the Roles of Pectin as an Active Participant in Plant Signaling Networks. *Plants, 10*(8), 1712.

So, P. T., & Dong, C. Y. (2001). Fluorescence spectrophotometry. *e LS*.

Somssich, M., Khan, G. A., & Persson, S. (2016). Cell wall heterogeneity in root development of Arabidopsis. *Frontiers in plant science, 7*, 1242.

Spirochrome. (2018). *Product information: Flipper-TR® (SC020)* [Datasheet]. https://spirochrome.com/documents/201901/datasheet_FLIPPER-TR_201906.pdf

Szymanski, W. G., Zauber, H., Erban, A., Gorka, M., Wu, X. N., & Schulze, W. X. (2015). Cytoskeletal components define protein location to membrane microdomains. *Molecular & Cellular Proteomics, 14*(9), 2493-2509.

Vaahtera, L., Schulz, J., & Hamann, T. (2019). Cell wall integrity maintenance during plant development and interaction with the environment. *Nature plants, 5*(9), 924-932.

van Munster, E. B., & Gadella, T. W. (2005). Fluorescence lifetime imaging microscopy (FLIM). In *Microscopy techniques* (pp. 143-175): Springer.

Wang, T., Zabotina, O., & Hong, M. (2012). Pectin–cellulose interactions in the Arabidopsis primary cell wall from two-dimensional magic-angle-spinning solid-state nuclear magnetic resonance. *Biochemistry, 51*(49), 9846-9856.

Wang, X. F., Periasamy, A., Herman, B., & Coleman, D. M. (1992). Fluorescence lifetime imaging microscopy (FLIM): instrumentation and applications. *Critical Reviews in Analytical Chemistry, 23*(5), 369-395.

Wickham, H. ggplot2: Elegant Graphics for Data Analysis. Springer-Verlag New York, 2016.

Yu, M., Cui, Y., Zhang, X., Li, R., & Lin, J. (2020). Organization and dynamics of functional plant membrane microdomains. *Cellular and Molecular Life Sciences, 77*(2), 275-287.

Yuan, F., Yang, H., Xue, Y., Kong, D., Ye, R., Li, C., . . . Krichilsky, B. (2014). OSCA1 mediates osmotic-stress-evoked Ca2+ increases vital for osmosensing in Arabidopsis. *Nature, 514*(7522), 367-371.

Zhang, B., Liu, K., Zheng, Y., Wang, Y., Wang, J., & Liao, H. (2013). Disruption of AtWNK8 enhances tolerance of Arabidopsis to salt and osmotic stresses via modulating proline content and activities of catalase and peroxidase. *International journal of molecular sciences, 14*(4), 7032-7047.

Zhou, J.-M., & Zhang, Y. (2020). Plant immunity: danger perception and signaling. *Cell, 181*(5), 978-989.

Zou, Y., Chintamanani, S., He, P., Fukushige, H., Yu, L., Shao, M., . . . Zhou, J. M. (2016). A gain-of-function mutation in Msl10 triggers cell death and wound-induced hyperaccumulation of jasmonic acid in Arabidopsis. *Journal of integrative plant biology, 58*(6), 600-609.

Appendix 1 – Excitation and emission spectra

An excitation and emission spectra was made of Flipper-TR, using HaCaT cells. Raw data in table A1.

Table A.1: Excitation and emission raw data, numbers represent intensity.

-1	-1	-1	-1	-1	210	68	42	31	23	20	565	
-1	-1	-1	-1	-1	134	65	43	32	24	21	560	
-1	-1	-1	-1	-1	96	58	40	31	23	19	555	
-1	-1	-1	-1	-1	92	64	46	36	27	21	550	
-1	-1	-1	-1	160	88	67	49	38	28	21	545	
-1	-1	-1	-1	142	106	84	65	51	36	26	540	
-1	-1	-1	-1	154	134	111	86	67	47	33	535	
-1	-1	-1	-1	184	176	150	117	91	62	43	530	
-1	-1	-1	246	212	212	182	140	108	73	50	525	
-1	-1	-1	245	256	262	227	175	135	89	61	520	
-1	-1	-1	262	306	317	276	212	162	107	73	515	
-1	-1	-1	260	322	336	292	224	171	112	77	510	
-1	-1	217	271	342	360	313	240	183	120	81	505	
-1	-1	228	337	432	461	401	307	233	151	101	500	
-1	-1	194	322	422	452	394	301	229	147	97	495	
-1	-1	241	408	540	578	504	385	292	186	122	490	
-1	174	216	377	507	544	476	365	278	178	117	485	
-1	102	157	286	390	424	377	290	222	140	92	480	
-1	55	99	184	251	276	247	191	146	93	61	475	
41	36	70	128	167	179	159	124	96	63	42	470	
495	514	533	552	571	590	609	628	647	666	685		Excitation
Emission												

Appendix 2 – Fluorescent lifetime of stress treated *Arabidopsis* seedlings

FLIM was used to find the fluorescent lifetime of Flipper-TR in the epidermal plasma membrane of *Arabidopsis* seedlings treated with either mock-, sorbitol-, ISX- or ISX + sorbitol treatment. See lifetimes in table A.2 and a line chart with mean lifetime and standard deviation for each treatment and timepoint in figure A.1.

Table A.2: Raw data of lifetimes (τ_1) from fitting of fluorescent decay, and χ2 (chi squared) value.

Stress	Time stressed (min)	τ_1	χ2
mock	5	4.19	1.058
mock	5	3.76	1.069
mock	5	3.667	1.096
sorbitol	60	3.57	1.099
sorbitol	60	3.699	1.056
sorbitol	60	3.756	1.062
mock	60	3.65	1.094
mock	60	3.768	1.122
sorbitol	90	3.604	1.2
sorbitol	90	3.879	1.127
sorbitol	90	3.868	1.09
sorbitol	120	3.777	1.061
sorbitol	120	3.738	1.039
sorbitol	120	3.6758	1.126
sorbitol	180	3.676	1.134
sorbitol	180	3.694	1.091
sorbitol	180	3.893	1.1
mock	180	3.317	1.108
mock	180	3.671	1.086
sorbitol	60	3.797	1.064
sorbitol	60	3.755	1.076
sorbitol	60	3.677	1.102
sorbitol	90	3.744	1.048

sorbitol	90	3.639	1.072
sorbitol	90	3.771	1.227
sorbitol	120	3.723	1.057
sorbitol	120	3.647	1.13
sorbitol	120	3.62	1.099
mock	5	3.688	1.088
mock	5	3.849	1.102
mock	5	3.549	1.095
sorbitol	180	3.687	1.158
sorbitol	180	3.546	1.07
sorbitol	5	3.648	1.08
sorbitol	5	3.719	1.027
sorbitol	5	3.59	1.083
sorbitol	5	3.467	1.032
sorbitol	5	3.92	1.021
sorbitol	5	3.797	1.017
sorbitol	5	3.51	1.013
sorbitol	60	3.555	1.053
sorbitol	60	3.543	0.997
sorbitol	60	3.666	1.057
mock	5	3.34	1.086
mock	5	3.479	1.045
mock	5	3.822	1.045
sorbitol	90	3.684	1.074
sorbitol	90	3.87	1.08
sorbitol	90	3.82	1.048
sorbitol	120	3.612	1.063
sorbitol	120	3.587	1.021
sorbitol	120	3.753	1.084
mock	60	3.473	1.067
mock	60	3.262	1.053
mock	60	3.697	1.044
mock	90	3.449	1.039

mock	90	3.483	1.066
mock	90	3.677	1.041
sorbitol	180	3.846	1.087
sorbitol	180	3.586	1.053
sorbitol	180	3.65	1.058
mock	120	3.66	1.083
mock	120	3.89	1.004
mock	120	3.574	1.065
mock	180	3.621	1.09
mock	180	3.37	1.081
mock	180	3.562	0.975
sorbitol	60	3.776	1.067
sorbitol	60	3.616	1.025
sorbitol	60	3.88	1.005
isx	5	3.477	1.017
isx	5	3.492	1.05
isx	5	3.395	1.05
isx	60	3.414	1.089
isx	60	3.804	1.078
isx	60	3.828	1.056
isx	90	3.613	1.015
isx	90	3.66	1.031
isx	90	3.463	1.076
isx	120	3.61	1.065
isx	120	3.501	1.083
isx	120	3.575	1.064
isx	180	3.617	1.081
isx	180	3.57	1.049
isx	180	3.468	1.065
sorbitol	5	3.826	1.012
sorbitol	5	3.834	1.054
sorbitol	5	4.27	1.001
mock	5	3.709	1.065

mock	5	3.854	1.014
mock	5	4.032	1.057
sorbitol	60	4.11	1.043
sorbitol	60	4.078	1.025
sorbitol	60	3.934	1.047
mock	60	4.132	1.032
mock	60	3.826	1.045
mock	60	3.764	1.071
sorbitol	90	3.873	1.022
sorbitol	90	4.24	1.065
sorbitol	90	3.889	1.06
mock	90	3.681	1.1
mock	90	3.826	1.089
mock	90	3.859	1.036
sorbitol	120	3.889	1.042
sorbitol	120	3.935	1.032
sorbitol	120	3.914	1.019
mock	120	3.878	1.096
mock	120	3.925	1.089
mock	120	3.796	1.045
sorbitol	180	4.001	1.054
sorbitol	180	3.829	1.027
sorbitol	180	3.741	1.066
mock	180	3.758	1.077
mock	180	3.82	1.084
mock	180	3.964	1.09
mock	5	3.579	1.071
mock	5	3.73	1.075
mock	5	3.738	1.025
isx	5	3.846	1.054
isx	5	3.763	1.021
isx	5	3.766	1.02
mock	60	3.935	1.038

mock	60	3.947	1.04
mock	60	3.79	1.094
isx	60	3.908	1.024
isx	60	3.72	1.092
isx	60	3.969	1.057
mock	90	3.564	1.036
mock	90	3.702	1.07
mock	90	3.775	1.088
isx	90	3.91	1.042
isx	90	3.758	1.069
isx	90	3.612	1.037
mock	120	3.68	1.044
mock	120	3.92	1.117
mock	120	3.415	1.08
isx	120	3.74	1.067
isx	120	3.959	1.094
isx	120	3.531	1.042
mock	180	3.729	1.016
mock	180	3.62	1.097
mock	180	3.59	1.031
isx	180	3.66	1.113
isx	180	3.777	1.058
isx	180	3.259	1.103
isx	5	3.901	1.032
isx	5	3.868	1.051
isx	5	3.84	1.011
mock	5	3.706	1.015
mock	5	3.725	1.022
mock	5	3.616	1.005
isx	60	3.812	1.023
isx	60	3.851	1.037
isx	60	3.675	1.012
mock	60	3.836	1.076

mock	60	3.803	1.062
mock	60	3.79	1.021
isx	90	3.706	1.029
isx	90	3.624	1.055
isx	90	3.657	1.077
mock	90	3.673	1.034
mock	90	3.764	1.083
mock	90	3.771	1.099
isx	120	3.69	1.077
isx	120	3.66	1.015
isx	120	3.894	1.127
mock	120	3.814	1.09
mock	120	3.64	1.054
mock	120	3.74	1.045
isx	180	3.65	1.139
isx	180	3.43	1.111
isx	180	3.364	1.128
mock	180	3.56	1.124
mock	180	3.825	1.047
mock	180	3.557	1.059
isx	240	3.62	0.002
isx	240	3.77	1.026
isx	240	3.47	1.074
mock	240	3.748	1.103
mock	240	3.763	1.032
mock	240	3.701	1.093
isx	240	3.628	1.059
isx	240	3.736	1.015
isx	240	3.53	1.054
mock	240	3.729	1.115
mock	240	3.77	1.058
mock	240	3.8	1.02
isx	300	3.594	1.033

isx	300	3.58	1.096
isx	300	3.548	1.074
mock	300	3.605	1.082
mock	300	3.549	1.071
mock	300	3.382	1.035
isx	300	3.66	1.096
isx	300	3.504	1.099
isx	300	3.485	1.077
mock	300	3.633	1.083
mock	300	3.689	1.098
mock	300	3.728	1.054
isx	360	3.431	1.044
isx	360	3.526	1.057
isx	360	3.522	1.088
mock	360	3.648	1
mock	360	3.45	1.061
mock	360	3.548	1.076
isx	360	3.41	1.117
isx	360	3.57	1.101
isx	360	3.45	1.113
mock	360	3.75	1.109
mock	360	3.595	1.076
mock	360	3.646	1.106
isx	420	3.496	1.116
isx	420	3.506	1.061
isx	420	3.36	1.105
mock	420	3.527	1.066
mock	420	3.749	1.068
mock	420	3.64	1.025
isx	420	3.455	1.09
isx	420	3.396	1.064
isx	420	3.381	1.117
mock	420	3.65	1.073

mock	420	3.692	1.068
mock	420	3.658	1.082
isx	480	3.68	1.096
isx	480	3.47	1.057
isx	480	3.319	1.104
mock	480	3.49	1.122
mock	480	3.349	1.068
mock	480	3.349	1.093
isx	480	3.36	1.011
isx	480	3.325	1.111
isx	480	3.353	1.109
mock	480	3.588	1.079
mock	480	3.6	1.062
mock	480	3.567	1.097
isx+sorb	180	4.051	1.033
isx+sorb	180	3.894	1.067
isx+sorb	180	3.999	1.057
isx+sorb	180	3.93	1.067
isx+sorb	180	3.861	1.079
isx+sorb	180	4.038	1.04
isx+sorb	180	3.842	1.051
isx+sorb	180	3.763	1.072
mock	180	3.958	1.043
mock	180	3.867	1.019
mock	180	3.678	1.101
isx	180	3.512	1.102
isx	180	3.839	1.028
isx	180	3.6	1.101
isx+sorb	300	3.791	1.054
isx+sorb	300	3.966	1.058
isx+sorb	300	3.855	1.019
isx+sorb	300	4.09	1.036
isx+sorb	300	3.97	1.032

isx+sorb	300	3.584	1.022
isx+sorb	300	3.228	1.078
isx+sorb	300	3.85	1.097
isx+sorb	300	3.9	1.074
mock	300	3.486	1.085
mock	300	3.5	1.054
mock	300	3.549	1.073
isx	300	3.607	1.089
isx	300	3.587	1.063
isx	300	3.573	1.053
isx+sorb	420	3.805	1.056
isx+sorb	420	3.844	1.107
isx+sorb	420	3.712	1.071
isx+sorb	420	4.037	1.072
isx+sorb	420	3.72	1.076
isx+sorb	420	3.629	1.033
isx+sorb	420	3.767	1.09
isx+sorb	420	3.773	1.04
isx+sorb	420	3.61	1.089
mock	420	3.467	1.078
mock	420	3.33	1.035
isx	420	3.486	1.025
isx	420	3.337	1.055
isx	420	3.497	1.064

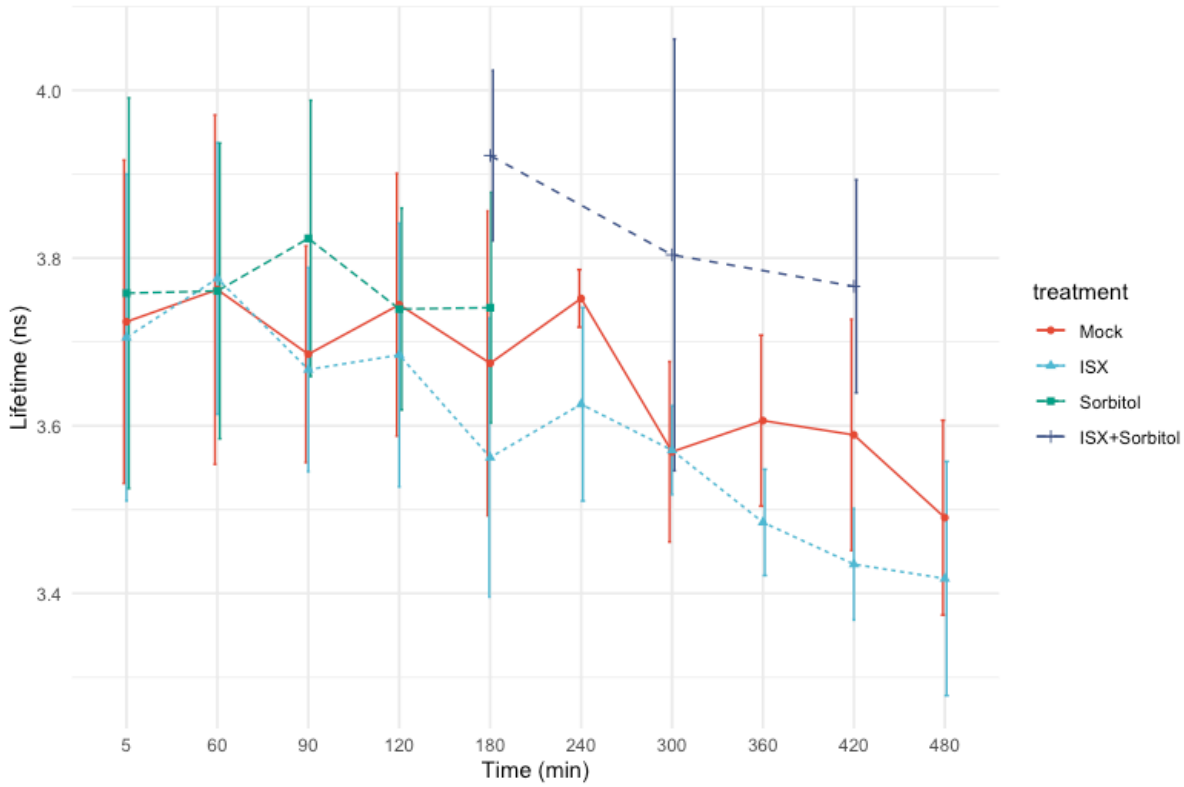

Figure A.1: Line chart of mean lifetime and standard deviation for each treatment and timepoint. Mock-treatment = red, ISX-treatment = light blue, sorbitol-treatment = green, ISX + sorbitol-treatment = dark blue.

Appendix 3 – Statistics

A one-way ANOVA and post hoc Tukey HSD was performed on the data to compare the different timepoint within the treatments and compare treatments at corresponding timepoints.

Mock treatment:

One-way ANOVA: p-value: 0.00675 **

Table A.3: P-values found with for different timepoints of mock-treatment found using a post-hoc Tukey HSD. Green cell signifies statistical significance.

	5	60	90	120	180	240	300	360	420
60	0.9996								
90	0.9997	0.9676							
120	1.0000	1.0000	0.9962						
180	0.9958	0.8829	1.0000	0.9775					
240	1.0000	1.0000	0.9980	1.0000	0.9908				
300	0.3583	0.1450	0.8237	0.2946	0.8480	0.4910			
360	0.8650	0.6059	0.9925	0.7812	0.9963	0.8587	1.0000		
420	0.6168	0.3180	0.9485	0.5202	0.9638	0.6850	1.0000	1.0000	
480	0.0754	0.0257	0.3222	0.0617	0.3298	0.1449	0.9952	0.9624	0.9795

ISX treatment

One-way ANOVA p-value: 1.85e-06 ***

Table A.4: P-values found with for different timepoints of ISX-treatment found using a post-hoc Tukey HSD. Green cell signifies statistical significance.

	5	60	90	120	180	240	300	360	420
60	0.9838								
90	0.9998	0.7970							
120	1.0000	0.9172	1.0000						
180	0.3518	0.0221	0.7669	0.5786					
240	0.9823	0.5419	0.9999	0.9981	0.9949				
300	0.5390	0.0612	0.8897	0.7532	1.0000	0.9989			
360	0.0826	0.0047	0.2676	0.1634	0.9794	0.7397	0.9705		
420	0.0027	0.0000	0.0185	0.0080	0.5218	0.2117	0.5225	0.9995	
480	0.0054	0.0002	0.0282	0.0137	0.5217	0.2181	0.5130	0.9974	1.0000

Sorbitol treatment

One-way ANOVA p-value: 0.742

Table A.5: P-values found with for different timepoints of sorbitol-treatment found using a post-hoc Tukey HSD.

	5	60	90	120
60	1.0000			
90	0.8946	0.8730		
120	0.9990	0.9974	0.7396	
180	0.9993	0.9982	0.7676	1.0000

ISX + sorbitol treatment

One-way ANOVA p-value: 0.198

Table A.6: P-values found with for different timepoints of ISX + sorbitol-treatment found using a post-hoc Tukey HSD.

	180	300
300	0.3740	
420	0.1921	0.8969

Comparing the different timepoints

Table A.7: P-value from one-way ANOVA and Post-hoc Tukey HSD for difference between treatments at same timepoint. Green cell signifies statistical significance.

Timepoint	One-way ANOVA p-value		ISX	Mock	Sorbitol
5 min	0.847	Mock	0.9727		
		Sorbitol	0.8414	0.9068	
60 min	0.98	Mock	0.9846		
		Sorbitol	0.9804	0.9997	
90 min	0.0265 *	Mock	0.9536		
		Sorbitol	0.0455	0.0587	
120 min	0.6	Mock	0.6199		
		Sorbitol	0.6694	0.9959	
180 min	0.000116 ***	Mock	0.2471		
		Sorbitol	0.0450	0.6996	
		ISX + Sorbitol	0.0001	0.0036	0.0779
240 min	0.0279 *	Mock	0.0279		
300 min	0.00719 **	Mock	0.9997		
		ISX + Sorbitol	0.0160	0.0151	
360 min	0.0327 *	Mock	0.0327		
420 min	1.28e-05 ***	Mock	0.0270		
		ISX + Sorbitol	0.0000	0.0105	
480 min	0.35	Mock	0.3500		

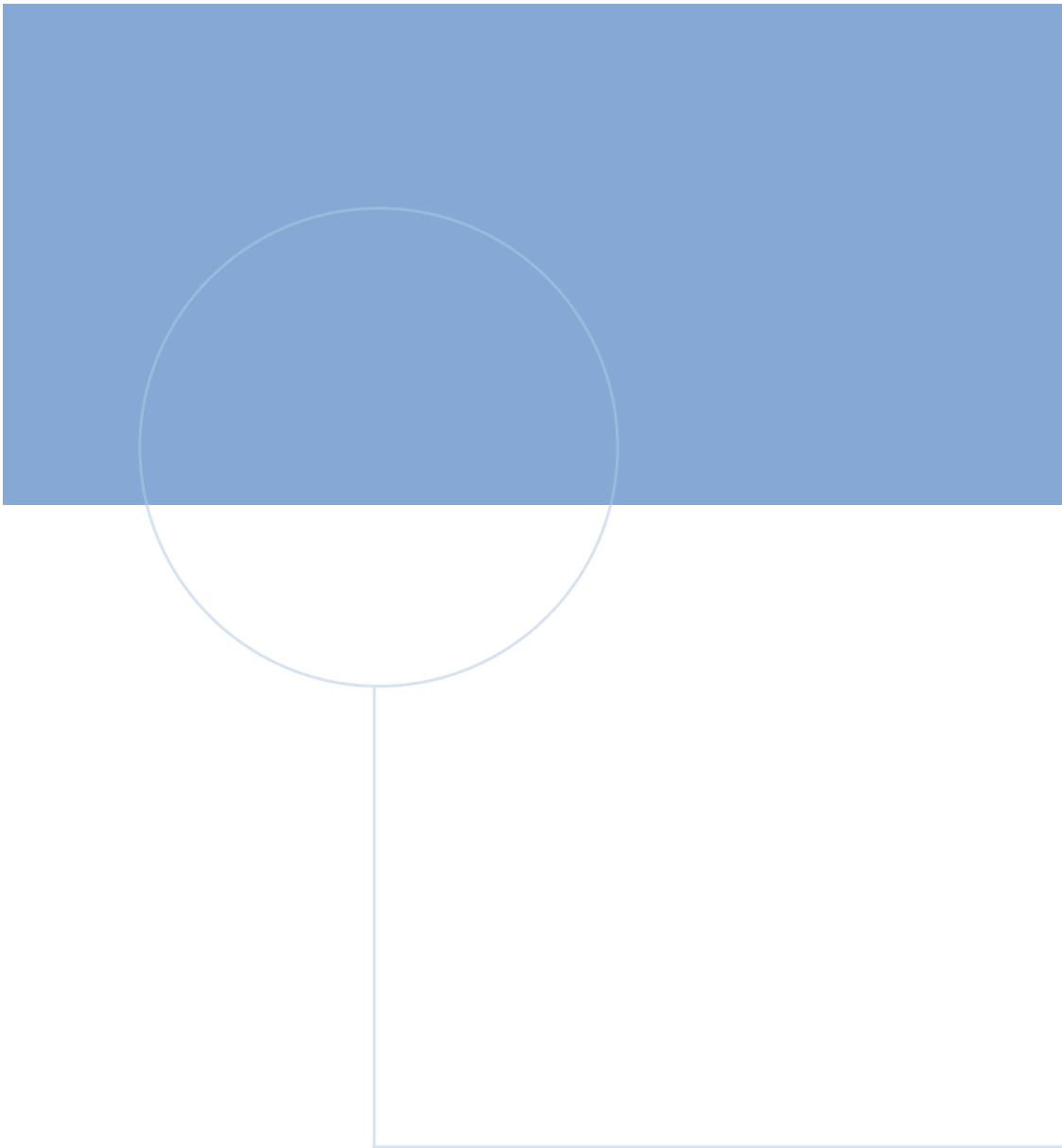

NTNU

Kunnskap for en bedre verden